PHASE PORTRAITS OF QUADRATIC SYSTEMS WITH FINITE MULTIPLICITY THREE AND A DEGENERATE CRITICAL POINT AT INFINITY

J.W. REYN AND X. HUANG

ABSTRACT. In this paper a quadratic system is meant to be the autonomous system of ordinary differential equations

$$\dot{x} = a_{00} + a_{10}x + a_{01}y + a_{20}x^2 + a_{11}xy + a_{02}y^2$$
$$\equiv P(x, y),$$
$$\dot{y} = b_{00} + b_{10}x + b_{01}y + b_{20}x^2 + b_{11}xy + b_{02}y^2$$
$$\equiv Q(x, y),$$

where $\cdot$ is defined to be d/dt and $a_{ij}, b_{ij} \in R$, and $P(x, y)$ and $Q(x, y)$ are relatively prime real polynomials, of degree at most two, which are not both linear. We study the class of quadratic systems with finite multiplicity three, consisting of systems with three elementary critical points, possibly complex or coinciding, and a degenerate type of critical point at infinity, being a point, which upon bifurcation such that only elementary critical points result, leaves one critical point in the finite part of the plane and two or three critical points at infinity. The notation for such a degenerate infinite critical point is $M_{1,2}^i$ and $M_{1,3}^i$, respectively.

A system with an $M_{1,3}^i$ point can be represented by the system
$$\dot{x} = \lambda x + \mu y + xy + y^2,$$
$$\dot{y} = x + y^2,$$

where $\lambda, \mu \in \mathbf{R}$, and 22 topologically different phase portraits are obtained.

A system with an $M_{1,2}^i$ point can be represented by the system
$$\dot{x} = \lambda x + \mu y + \gamma xy + \delta(x + y^2),$$
$$\dot{y} = x + y^2,$$

where $\mu, \gamma, \delta \in \mathbf{R}$ whereas $\lambda \in \{0, 1\}$ and $\gamma \notin \{0, 1\}$. As a result of the classification, 119 topologically different phase portraits are obtained.

In all systems discussed in this paper, there exists at most
one limit cycle and, if it exists, it is hyperbolic.

1. Introduction. In this paper by a quadratic system is meant the
autonomous system of ordinary differential equations

$$\dot{x} = a_{00} + a_{10}x + a_{01}y + a_{20}x^2 + a_{11}xy + a_{02}y^2 \equiv P(x,y),$$
$$\dot{y} = b_{00} + b_{10}x + b_{01}y + b_{20}x^2 + b_{11}xy + b_{02}y^2 \equiv Q(x,y),$$

where $\cdot$ is defined to be d/dt, $a_{ij}, b_{ij} \in R$, and $P(x,y), Q(x,y)$ are
relatively prime real polynomials, of degree at most two, which are
not both linear. In a way, quadratic systems may be considered
to be the first class of systems, which presents itself if a step away
from linear systems into the field of nonlinearity is desired. In fact,
in the qualitative theory of ordinary differential equations, quadratic
systems were given ample attention, which led to an increasing flow
of papers on the subject [15]. Apart from the value of developing a
theoretical body of knowledge as a means in itself, great importance
should also be attached to the impact the acquired knowledge has
in various fields of application. In a survey of the present situation,
it may be observed that the search for periodic solutions—it being
important and difficult to trace elements of such portraits—has had
a profound influence on the structure of what is known about the
phase portraits of quadratic systems. As a result, the phase portraits
with an infinite number of periodic solutions around center points are
known in a highly ordered way [20], and the corresponding conditions
on the coefficients in (1) are given in affine invariant form [4]. Many
results are also known about existence, uniqueness and simultaneous
occurrence of limit cycles in systems either characterized by giving a
system in its analytical form as, for instance, given in the classification
of Ye Yanqian, or by having certain properties, such as containing weak
or multiple critical points [21]. Nevertheless, various other classes, not
necessarily containing periodic solutions, such as homogeneous systems,
systems with algebraic solution curves and various systems encountered
in applications, were also investigated, leading to information on phase
portraits.

In classifying all possible phase portraits of quadratic systems, with
the additional aim of obtaining a quick reference for those working in
applications, it seems natural to start, as is usually done in the analysis

of a particular phase portrait, by investigating the possible number, relative location and character of (finite and infinite) critical points in such systems and use their various possible combinations to define classes of quadratic systems. This was done by Reyn [**16, 17**], who defined 170 subclasses grouped together in five classes of equal finite multiplicity. Here the *finite multiplicity m_f of a quadratic system* is defined to be the sum of the multiplicities of the (real and complex) finite critical points of the system. The multiplicity of a critical point is understood in the usual sense as the number of common zeros of $P(x, y) = 0$ and $Q(x, y) = 0$ in that critical point (see, e.g., [**2**, p. 65]). If the number of critical points of a quadratic system is finite, it has at most four critical points, which then are elementary and $m_f = 4$. This remains to be the case also if, by changing the coefficients in the differential equations the critical points are made to coincide or to become complex, as long as the critical points remain in the finite part of the plane. Lowering the finite multiplicity may be obtained by changing the coefficients such that one or more finite critical points have moved to infinity. Then, for a quadratic system $0 \le m_f \le 4$. Since there are up to three possible locations of infinite critical points, lowering the finite multiplicity m_f of a quadratic system will increase the complexity and multiplicity (up to seven) of these points and at the same time decrease the number of parameters in the system as well as the number of phase portraits. In fact, the classification of phase portraits for $m_f = 0$ was made by Reyn [**18**] and 27 topologically different phase portraits were found; trivially, none of them containing a limit cycle. The classification for $m_f = 1$ was also given by Reyn [**19**], leading to 38 phase portraits, and it was shown that a phase portrait in this class contains at most one limit cycle. Work is in progress on the classification $m_f = 2$. For it appears that in this class a phase portrait can have at most two limit cycles. In fact, proofs are available to show this phenomenon, except for one case, wherein there is a strong numerical evidence of this property. Further evidence through known cases for $m_f = 3$ suggests that there are at most three limit cycles for this class, whereas all known examples of quadratic systems with (at least but possibly at most) four limit cycles have two real and two complex critical points and thus belong to $m_f = 4$. This led to the conjecture (Reyn [**19**]), that the number of limit cycles in a quadratic system is at most equal to its finite multiplicity m_f. Apart from trying to prove this conjecture for $m_f = 3$, this class is also interesting in itself,

and some subclasses have already been studied from other aspects. For instance, most of the bounded quadratic systems, as introduced by Dickson and Perko in 1970 [**9**] and subsequently given attention by various authors [**6, 5**], belong to $m_f = 3$. An interesting new class of quadratic systems, also belonging to $m_f = 3$, was recently studied by Coppel [**7**] in response to a problem encountered in the study of the shear flow between parallel plates of a non-Newtonian fluid [**13**]. Another application, resulting in an equation in the class $m_f = 3$, was given by Hulshof [**12**], who studied similarity solutions of the porous medium equation with sign changes.

In a systematic approach to investigate the phase portraits of $m_f = 3$ we start with the simplest case, being characterized by the most complicated infinite critical point that can occur in $m_f = 3$. A multiple infinite critical point will be indicated by $M_{p,q}^i$, where i indicates the index of the point, p the maximum number of finite critical points and q the maximum number of infinite critical points that can bifurcate from it upon arbitrary changes in the coefficients of the differential equation. If $p \neq 0$, the point is transversally (with respect to the Poincaré circle) nonhyperbolic, and for $m_f = 3$ there is one such point and $p = 1$. The most complicated infinite critical point is then an $M_{1,3}^i$, being, in fact, a fourth order saddle node with index 0, and the only critical point at infinity possible in the systems that will first be studied. Thereafter, systems with an $M_{1,2}^i$ type of infinite critical point will be studied. It follows that these systems also have an elementary saddle point at infinity. Letting this point coincide with $M_{1,2}^i$ again yields the class with an $M_{1,3}^i$ point. The remaining class to be studied has an $M_{1,1}^0$ critical point at infinity. This is a far more elaborate class, containing in fact also the bounded quadratic systems in $m_f = 3$. The limit cycle problem for this class appears to be more involved [**11**].

2. Quadratic systems with finite multiplicity 3 and an $M_{1,3}^i$ type of critical point at infinity. Critical points of (1) are located at the intersection points of $P(x,y) = 0$ and $Q(x,y) = 0$, being the ∞ and 0 isoclines, respectively, and sending such a point to infinity in a certain direction makes this direction a common asymptotic direction of the conics $P(x,y) = 0$ and $Q(x,y) = 0$, so that the quadratic terms in (1) have a common linear factor. Without loss of generality, this factor may be taken to be y, so that $a_{20} = b_{20} = 0$ can be taken,

yet, since $m_f = 3$ is obtained from the class $m_f = 4$ by sending only one critical point to infinity, there is only one common linear factor so $c_{56} \equiv a_{11}b_{02} - a_{02}b_{11} \neq 0$. Since, moreover, an infinite critical point of (1) is in the same direction, given by $y = ux$, as the flow on the solution curves approaching it, u should be a solution of

$$f(u) = a_{02}u^3 + (a_{11} - b_{02})u^2 + (a_{20} - b_{11})u - b_{20} = 0,$$

with $a_{20} = b_{20} = 0$. For $u = 0$ to be a point of third order tangent to the Poincaré circle, then $b_{11} = 0$, $b_{02} = a_{11} \neq 0$, since $c_{56} = a_{11}^2 \neq 0$, whereas, further, there should be $a_{02} \neq 0$. Also, it may be seen that for $m_f = 3$ there exists at least one real critical point in the finite part of the plane, which then may be thought to be located at the origin, thus we may put $a_{00} = b_{00} = 0$. For (1) we may then write

$$(2) \qquad \begin{aligned} \dot{x} &= a_{10}x + a_{01}y + a_{11}xy + a_{02}y^2 \equiv P(x,y), \\ \dot{y} &= b_{10}x + b_{01}y + a_{11}y^2 \equiv Q(x,y), \end{aligned}$$

with $a_{11} \neq 0$, $a_{02} \neq 0$, and we may take $a_{11} = a_{02} = 1$ if needed by replacing x by $a_{02}x$, y by $a_{11}y$ and $a_{11}^2 t$ by t. Furthermore, if $b_{10} = 0$, there are at most two roots of $Q(x,y) = 0$ and, correspondingly, at most two roots of $P(x,y) = 0$, thus $m_f \leq 2$. Thus, $b_{10} \neq 0$, and we may take $b_{10} = 1$ if needed by replacing x by $b_{10}x$, y by $b_{10}y$ and $b_{10}t$ by t. Finally, by replacing $x + b_{01}y$ by x, the system takes the form

$$(3) \qquad \begin{aligned} \dot{x} &= \lambda x + \mu y + xy + y^2, \\ \dot{y} &= x + y^2, \end{aligned}$$

with $\lambda, \mu \in R$, which is of the class $m_f = 3$ and has an infinite critical point $M_{1,3}^i$ "at the ends of the x-axis."

The conditions on the coefficients of (1) such that a system belongs to the class studied in this section are given in the Appendix.

3. Phase portraits of quadratic systems in the class $m_f = 3$ having an $M_{1,3}^i$ type of critical point at infinity. According to Theorem C in Coppell [**8**], the system (3) has at most one limit cycle since the highest degree terms of P and Q are both divisible by the highest degree terms of the divergence $P_x + Q_y$ and, if this limit cycle exists, it is hyperbolic.
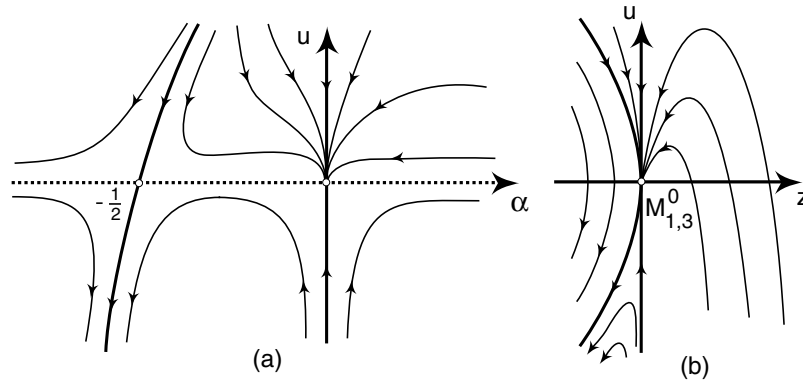
FIGURE 1. The fourth order saddle node $M_{1,3}^0$ at infinity.

In order to analyze $M_{1,3}^i$, we use the Poincaré transformation $z = x^{-1}$, $u = yx^{-1}$, then (3) becomes after a scaling of time

$$
\begin{aligned}
\dot{z} &= -z(\lambda z + u + \mu z u + u^2), \\
\dot{u} &= z - \lambda z u - \mu z u^2 - u^3,
\end{aligned}
$$
(4)

and $M_{1,3}^i$ is located in $z = u = 0$. For the blow up we use the transformation $z = u^2 \alpha(t)$ to obtain

$$
\begin{aligned}
\dot{\alpha} &= \alpha u(-1 - 2\alpha + u + \lambda \alpha u + \mu \alpha u^2), \\
\dot{u} &= u^2(\alpha - u - \lambda \alpha u - \mu \alpha u^2).
\end{aligned}
$$
(5)

By putting $u \, dt = d\tau$, system (5) is replaced by a system which on $u = 0$ has critical points at $\alpha = 0$ and $\alpha = -1/2$; they can be shown to be a second order saddle node and a saddle, respectively. The solution curves near $u \equiv 0$ can now be easily determined and are shown in Figure 1a. Returning to the z, u plane yields Figure 1b, which shows a fourth order saddle node $M_{1,3}^0$, having hyperbolic sectors with opening angles 0 and π in the half plane $z < 0$ and a parabolic sector with opening angle π for $z > 0$, partly extending into $z < 0$. It should be remarked that the only orbits approaching the critical point with a curvature different from zero are the separatrices in $z < 0$. This fact will be explored later since their curvature at $z = u = 0$ equals that of the parabolic orbits of (3) for those values of λ and μ for which they
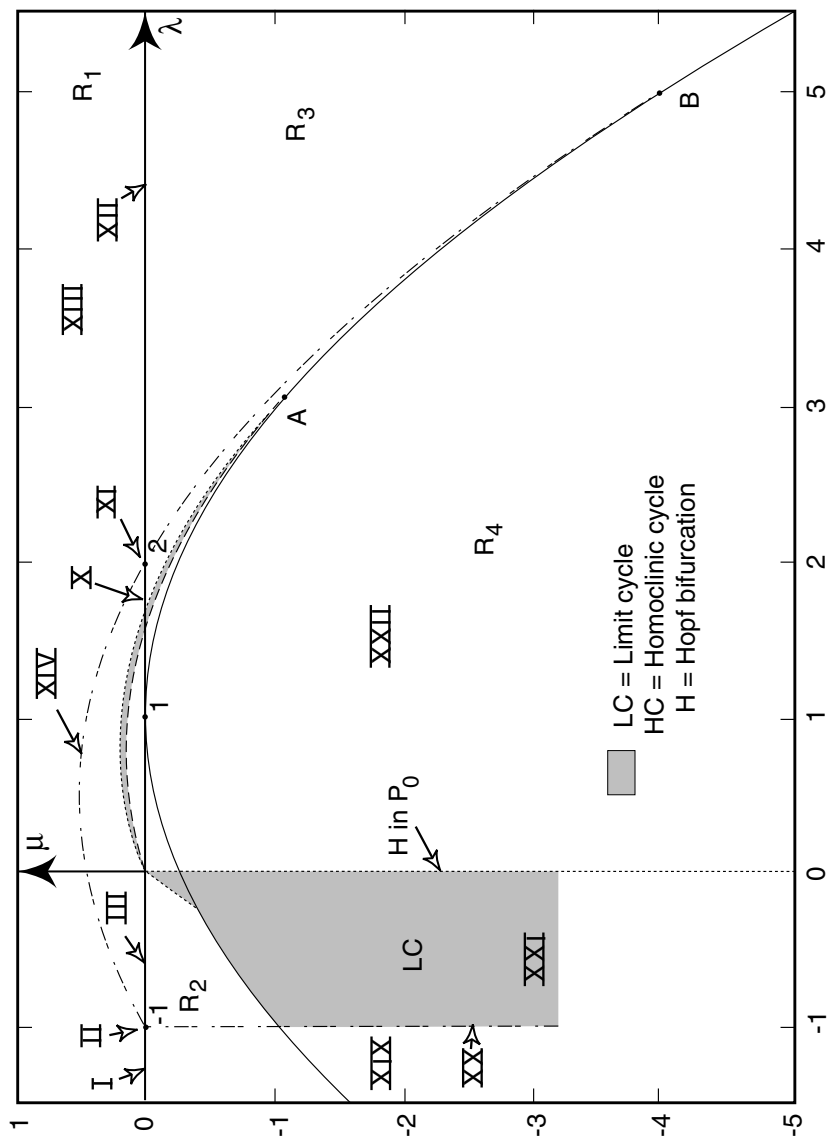
FIGURE 2. Parameter plane λ, μ with bifurcation curves.

FIGURE 2. (Close-up) Parameter plane λ, μ with bifurcation curves.

exist, these orbits being given by the expressions

(6)
$$x = -\frac{1}{2}\mu - y - \frac{1}{2}y^2,$$
$$\lambda \equiv -1, \quad -\infty < \mu < \infty,$$

(7)
$$x = \frac{1}{3}(\lambda - 2)y - \frac{1}{2}y^2, \quad -\infty < \lambda < \infty,$$
$$\mu = -\frac{2}{9}(\lambda + 1)(\lambda - 2).$$

The significance of these orbits for the phase portraits of (3) will be discussed later.

We will now investigate the finite part of the phase plane. Apart from the critical point P_0 in $(0,0)$, there exist the critical points P_+ with coordinates $x_+ = -y_+^2$, $y_+ = (1/2)(1 - \lambda + \sqrt{(1-\lambda)^2 + 4\mu})$, and P_- with coordinates $x_- = -y_-^2$, $y_- = (1/2)(1 - \lambda - \sqrt{(1-\lambda)^2 + 4\mu})$. Obviously, for $\mu < -(1/4)(1 - \lambda)^2$, P_+ and P_- are complex points; for $\mu = (-1/4)(1 - \lambda)^2$, P_+ and P_- coincide; for $\mu = 0$, $\lambda \leq 1$, P_0 and P_- coincide; for $\mu = 0$, $\lambda \geq 1$, P_0 and P_+ coincide; and for all other values of (λ, μ), there exist three real (elementary) critical points. Correspondingly, as is indicated in Figure 2, we distinguish in the λ, μ plane the regions $R_1 : \mu > 0$; $R_2 : \lambda < 1$, $(-1/4)(1 - \lambda)^2 < \mu < 0$; $R_3 : \lambda > 1$, $(-1/4)(1 - \lambda)^2 < \mu < 0$; and $R_4 : \mu < (-1/4)(1 - \lambda)^2$. In determining the phase portraits, not all values of (λ, μ) need be considered, since all portraits with three elementary critical points occur for values of (λ, μ) in either R_1, R_2 or R_3. This may be seen as follows. Let (x_*, y_*) represent either P_+ or P_- and replace in (3) x by $-x_* - 2y_*^2 + x + 2yy_*$ and y by $-y_* + y$ then the origin is shifted to (x_*, y_*) and (3) takes the form

$$\dot{x} = (\lambda + 3y_*)x + [\mu + 2y_*(1 - \lambda - y_*) + x_*]y + xy + y^2,$$
$$\dot{y} = x + y^2,$$

which is of the same form as (3) with different values for the parameters. The mapping $\lambda \leftrightarrow \lambda + 3y_*$, $\mu \leftrightarrow \mu + 2y_*(1 - \lambda - y_*) + x_*$ then determines the mapping $R_1 \leftrightarrow R_2$ if $(x_*, y_*) = (x_-, y_-)$ and $R_1 \leftrightarrow R_3$ if $(x_*, y_*) = (x_+, y_+)$. As a result, we may restrict our attention to $\mu \geq 0$ and $\mu < (-1/4)(1 - \lambda)^2$. We begin the analysis with $\mu = 0$.
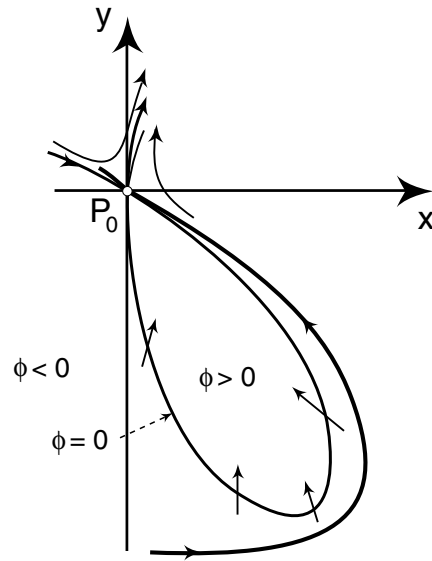
FIGURE 3. Relative location of the unbounded separatrix cycle for $\lambda = \lambda_{II} = -1$, $\mu = 0$ and regions of rotated vector fields.

We may summarize the statements above in

Property 1. *System* (3) *has the following properties*:

(i) *the only infinite critical point of* (3) *is a fourth order saddle node* $M_{1,3}^0$*, the separatrices of which extend into the finite part of the plane having the same curvature as the parabolic orbits of* (3)*, for those values of* λ *and* μ *where these orbits exist,*

(ii) *there exist parabolic orbits of* (3)*; they are given by* (6) *and* (7)*,*

(iii) *the phase portraits with one real critical point and two complex critical points can be determined by taking* $\mu < (-1/4)(1 - \lambda)^2$*; those with two real critical points by taking* $\mu = 0$ *and those with three real critical points by taking* $\mu > 0$*,*

(iv) *system* (3) *has at most one limit cycle and, if it exists, it is hyperbolic.*

I :$-\infty < \lambda < -1$

II :$\lambda = -1$

III : $-1 < \lambda < 0$

IV :$\lambda = 0$

V :$0 < \lambda < 1$

VI :$\lambda = 1$

VII :$1 < \lambda \leq \frac{3}{2}$

VIII :$\frac{3}{2} < \lambda < \lambda_{\mathrm{IX}}$

IX : $\lambda = \lambda_{\mathrm{IX}}$

X :$\lambda_{\mathrm{IX}} < \lambda < 2$

XI :$\lambda = 2$

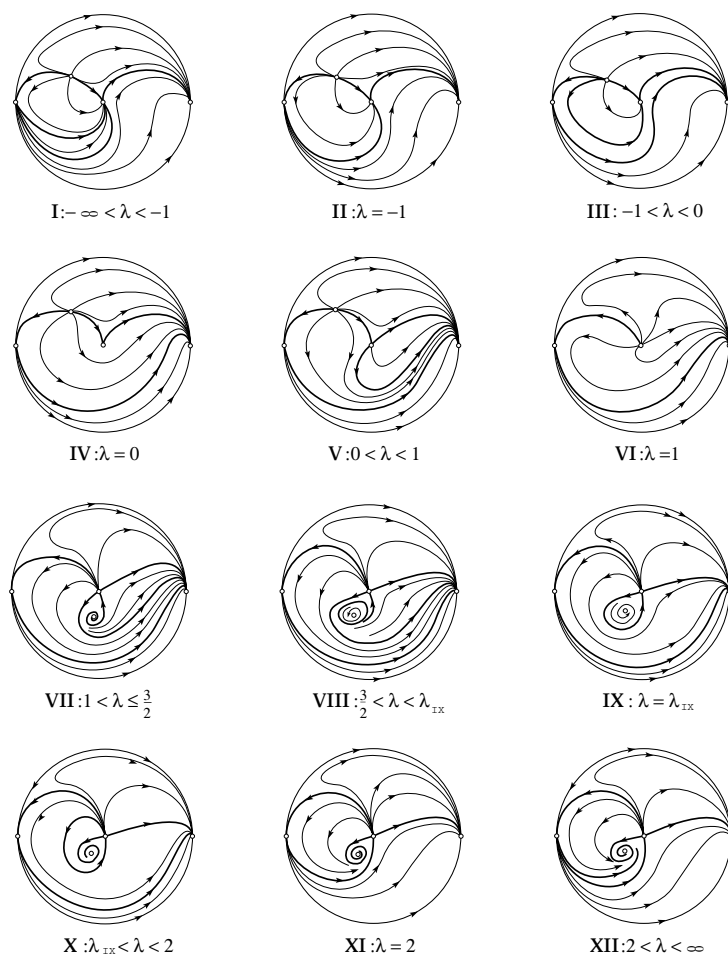**XII** :$2 < \lambda < \infty$

FIGURE 4. Phase portraits for $\mu = 0$.

3.1. Phase portraits for $\mu = 0$**.** The phase portraits for $\mu = 0$
are given in Figure 4 I–XII, and the corresponding values for λ are
indicated in Figure 2. For $\lambda < 1$, P_- coincides with P_0, for $\lambda = 1$, both
P_- and P_+ coincide with P_0, and for $\lambda > 1$, P_+ coincides with P_0. So,
for $\lambda \neq 1$, P_0 is a second order critical point with eigenvalues 0 and λ,
as a result of which, P_0 is a second order saddle node for $\lambda \neq 0(\neq 1)$
and a second order cusp point for $\lambda = 0$, both with index 0, so that the
remaining elementary point is an antisaddle. For $\lambda = 1$, P_0 is a third
order node, having index 1. Further details on these types of critical
points may be obtained using Theorems 65 and 67 in [**1**]. For either the
antisaddle P_+ or P_- it may be found that div $(P, Q) = 3 - 2\lambda$. So P_+,
occurring for $\lambda < 1$, is unstable, whereas P_- is unstable for $1 < \lambda < 3/2$
and stable for $\lambda > 3/2$. As a result of the change of stability, a limit
cycle is bifurcated at $\lambda = 3/2$, persisting on the interval $3/2 < \lambda < \lambda_{IX}$
for some λ_{IX} yet to be discussed.

Knowing enough properties of the critical points and using continuity
arguments possible phase portraits may now be drawn, except that
the relative location of separatrices still have to be determined. With
the help of numerical calculations and the theory of rotated vector
fields, for which the reader is referred to [**21, 10, 14**], it may be
shown, however, that the separatrix structure is as shown in Figure 4.
Numerical calculations show that, for $\lambda = -2$ the structure is, as in
Figure 4 I, whereas for $\lambda = -0.5$ that in Figure 4 III is obtained. For
$\lambda < 0$, replacing x by $-\lambda^3 x$, y by $\lambda^2 y$ and t by $-\lambda^{-1}t$, (3) with $\mu = 0$
takes the following form

$$\dot{x} = -x - \lambda xy + y^2 \equiv R(x, y),$$
$$\dot{y} = x - \lambda y^2 \equiv S(x, y),$$

so that $R(\partial S/\partial \lambda) - S(\partial R/\partial \lambda) = -y\phi(x, y)$ where $\phi(x, y) = -x^2 -
xy + y^3$. The curve $\phi(x, y) = 0$ is illustrated in Figure 3, enclosing
in the fourth quadrant an oval region, wherein $\phi > 0$. In the case
that in the lower half plane the separatrix from the infinite critical
point and the saddle node coincide, as illustrated in Figure 4 II, this
separatrix approaches the origin along $y = -x - x^2/2 + o(x^2)$, so that
along it $\dot{\phi} = x^3/2 + o(x^3) > 0$ and $\phi < 0$ on it, since $\phi(0, 0) = 0$
and the separatrix cannot cross $\phi = 0$ in the lower half plane, since
$\dot{\phi}_{\phi=0} = y^2(x - \lambda y^2) > 0$. This separatrix is therefore in the region,
wherein $-y\phi(x, y) < 0$, so that changing λ breaks it up in a unique

way, which shows that it is unique, and occurs at some value $\lambda = \lambda_{II}$, where $-2 < \lambda_{II} < -0.5$. In fact, it can be shown, using the parabolic solutions (6) and (7) with $\mu = 0$ that $\lambda_{II} = -1$. This may be seen as follows. According to property 1(ii), for $\mu = 0$ there exists a parabolic solution if $\lambda = -1$, which then coincides with the separatrices of the infinite critical point, since they are the only orbits approaching this point with the same curvature as the parabola. Since the parabola has a continuously changing tangent, the phase portrait in Figure 4II is then the only candidate for $\lambda = -1$, since in Figure 4I there is discontinuity at $x = y = 0$. We may check that P_+ is on the parabola, since $P_+ = (-4, 2)$ is located on $x = -y - y^2/2$.

In a similar way, the theory of rotated vector fields may be used to show the uniqueness of a homoclinic cycle at some value $\lambda = \lambda_{IX} \approx 1.65$ as illustrated in Figure 4 IX. For this we use the substitutions $x \to \lambda^3 x$, $y \to \lambda^2 y$ and $t \to \lambda^{-1} t$. The limit cycle generated at $\lambda = 3/2$ will be absorbed in this homoclinic cycle. There is also a unique unbounded separatrix cycle, as illustrated in Figure 4 XI. Using similar arguments as for Figure 4 II, it can be shown that $\lambda_{XI} = 2$ and that the unbounded separatrix cycle is given by $x = -(1/2)y^2$.

3.2. Phase portraits for $\mu > 0$. The phase portraits for $\mu > 0$ are given in Figure 5 XIII–XVIII, and the corresponding regions in the λ, μ plane are indicated in Figure 2. As for $\mu = 0$, P_+ is located in the upper half plane and P_- in the lower half plane; however, they now occur simultaneously. They are both antisaddles, since the sum of the indices of all critical points is equal to 1, and P_0 is a saddle, as the product of the eigenvalues in P_0 equals $-\mu < 0$. The antisaddle P_+ is unstable, since in it

$$\operatorname{div}(P, Q) = \lambda + 3y_* = \frac{1}{2}\left[3 - \lambda + 3\sqrt{(1 - \lambda)^2 + 4\mu}\right] > 0.$$

The antisaddle P_- changes its stability at $0 < \lambda < 3/2$, $\mu = \lambda/3 - (2/9)\lambda^2$, being unstable for $0 < \lambda < 3/2$, $0 < \mu \leq \lambda/3 - (2/9)\lambda^2$ and stable for all other values of λ and $\mu > 0$. As a result, an unstable limit cycle is generated in a Hopf bifurcation, when crossing the fine focus curve for P_- from the unstable to the stable region in the λ, μ plane. The phase portrait corresponding to $0 < \lambda < 3/2$, $0 < \mu \leq 1/3 - (2/9)\lambda^2$ is given in Figure 5 XVIII and that with the
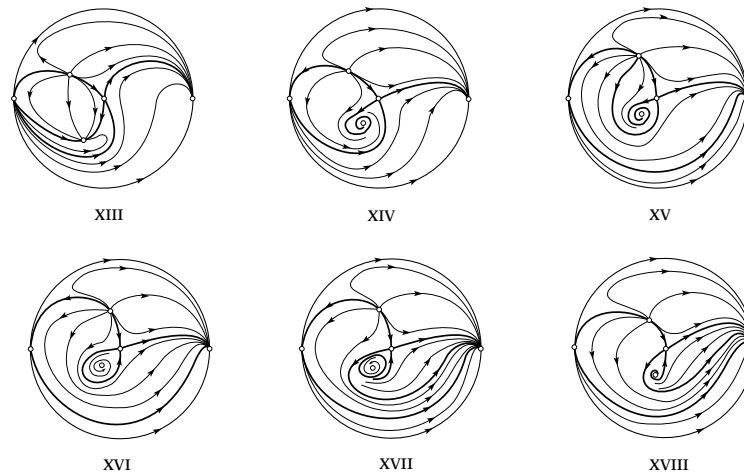
FIGURE 5. Phase portraits for $\mu > 0$.

(unique) limit cycle in Figure 5 XVII. For $\mu > 0$, the region in the λ, μ plane corresponding to the existence of a limit cycle is bounded above by a curve representing a homoclinic cycle; the phase portrait for the latter case being given in Figure 5 XVI. The uniqueness of this homoclinic cycle may again be shown using the theory of rotated vector fields. The curve in Figure 2 for the homoclinic cycle was found by numerical calculations. Just above the curve for the homoclinic bifurcation and also adjacent to the part of the axis indicated by III and X, the phase portrait is as given in Figure 5 XV, whereas for large enough values of μ and also adjacent to the part of the λ axis indicated by I and XII the phase portrait is as given in Figure 5 XIII. It can be shown, using the theory of rotated vector fields, that there is a unique curve in the λ, μ plane, separating regions XIII and XV, representing Figure 5 XIV, wherein in the lower half plane the separatrix of the infinite critical point coincides with a separatrix of the saddle point. This curve is given by $\mu = (-2/9)(\lambda + 1)(\lambda - 2)$ and the separatrices, connecting P_0, P_+ and $M_{1,3}^0$ by $x = (1/3)(\lambda - 2)y - (1/2)y^2$. This may be seen using property 1(ii) similarly as for Figures 4 II and XI. The parabolic orbit $x = -\mu/2 - y - y^2/2$ for $\lambda \equiv -1$, $\mu > 0$, so in

region XIII, coincides with the separatrices through $M_{1,3}^0$ and an orbit connecting P_- and P_+ to the left of P_0.

Since for $\lambda = \mu = 0$ (3) has a cusp at the origin, for small values of λ and μ the bifurcation diagram of Figure 2 should be obtainable from the values of the Bogdanov-Takens bifurcation. Replacing $3\lambda + 9y$ by x, $27(x + y^2)$ by y, and $t/3$ by t, (3) is obtained in the form, used by Bogdanov [3]

$$
(8) \qquad \begin{aligned} \dot{x} &= y, \\ \dot{y} &= \alpha + \beta x + x^2 + xy - \gamma x^3, \end{aligned}
$$

where $\alpha = 3(3\lambda^2 - 9\lambda\mu - 2\lambda^3)$, $\beta = 3(3\mu - 2\lambda + \lambda^2)$, $\gamma = 1/9$. From [3], it follows that a weak focus occurs for $\alpha = 0$ and, in particular, that P_0 is a weak focus for $\mu < 0$, $\lambda = 0$, P_- is a weak focus for $\mu = (1/3)\lambda - (2/9)\lambda^2$, where λ and μ should be small. The homoclinic bifurcation curve enters $(0,0)$ according to $\alpha \approx (-6/25)\beta^2$, corresponding to $\mu \approx (7/3)\lambda$ for $\lambda < 0$ and $\mu \approx (7/18)\lambda$ for $\lambda > 0$.

The mapping $R_1 \to R_2$ yields that the curve corresponding to Figure 5 XIV is mapped onto $\lambda \equiv -1$, $-1 < \mu < 0$, whereas the mapping $R_1 \to R_3$ gives that this curve is mapped onto $\mu = (-2/9)(\lambda+1)(\lambda-2)$, $2 < \lambda < 5$.

3.3. Phase portraits for $\mu < (-1/4)(1-\lambda)^2$. For $\mu < (-1/4)(1-\lambda)^2$, P_+ and P_- are complex critical points and P_0 is the only real critical point, which then must be an antisaddle, unstable for $\lambda > 0$, stable for $\lambda < 0$. For $\lambda > 0$ the phase portrait is given in Figure 6 XXII; there is no limit cycle. Lowering the value of λ leads to the bifurcation of an unstable limit cycle at $\lambda = 0$ as illustrated in Figure 6 XXI, which at some value of $\lambda = \lambda(\mu)$, is absorbed in an unbounded separatrix cycle as illustrated in Figure 6 XX. Further lowering of λ leads to the separatrix structure as given in Figure 6 XIX. The unbounded separatrix cycle may be shown to be unique, again, by using the theory of rotated vector fields. Moreover, using the lemma again, the unbounded separatrix cycle may be seen to be given by $x = -\mu/2 - y - y^2/2$, $\lambda \equiv -1$, $-\infty < \mu < -1$. Because of the possibility of the mappings $R_1 \leftrightarrow R_2$, $R_1 \leftrightarrow R_3$, the λ axis can be mapped onto the curve $\mu = -(1 - \lambda^2)/4$ and the phase portraits in Figure 6 may be obtained by bifurcating the phase portraits in Figure 4.
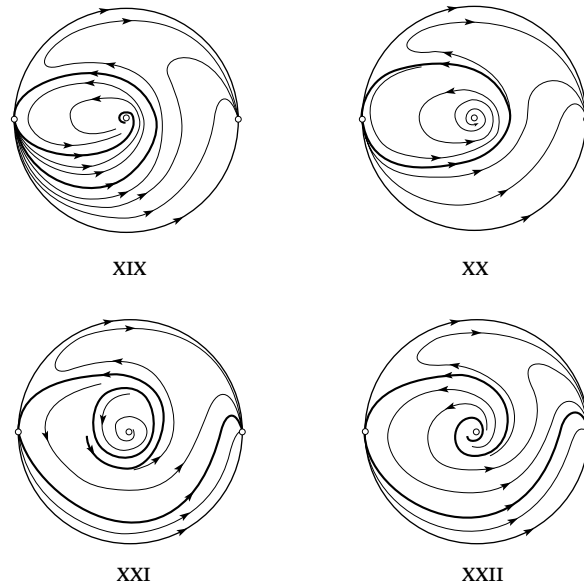
FIGURE 6. Phase portraits for $\mu < -(1/4)(1 - \lambda)^2$.

3.4. Conclusion. As a result of the analysis in Section 3, we now may state

Theorem 1. *For the class of quadratic systems with finite multiplicity $m_f = 3$ and an $M_{1,3}^i$ type of infinite critical point, this point is a nilpotent fourth order saddle node $M_{1,3}^0$, and the conditions on the coefficients in the system such that it belongs to this class are given in the Appendix. Moreover, the class may be represented by the system*

$$\dot{x} = \lambda x + \mu y + xy + y^2,$$
$$\dot{y} = x + y^2,$$

where $\lambda, \mu \in \mathbf{R}$. The 22 topologically different phase portraits are given in Figures 4, 5 and 6, corresponding to $\mu = 0$, $\mu > 0$ and $\mu < (1-\lambda)^2/4$, respectively, and the points in the λ, μ parameter plane corresponding to these phase portraits are indicated in Figure 2. System (3) has at most one limit cycle and, if it exists, it is hyperbolic.

4. Quadratic systems with finite multiplicity 3 and an $M_{1,2}^i$ type of critical point at infinity. The consideration given in Section 2 to show that equation (3) represents the quadratic systems of class $m_f = 3$ with an infinite critical point of type $M_{1,3}^i$ at the ends of the x axis may be repeated to obtain a similar result for the class $m_f = 3$ with an infinite critical point of type $M_{1,2}^i$ at the ends of the x axis. Starting again with equation (1), imposing the same conditions, with the difference that now at $u = 0$ there is a point of second order tangent to the Poincaré circle, thus $b_{11} = 0$, $a_{11} \neq b_{02}$, leads to

$$\dot{x} = a_{10}x + a_{01}y + a_{11}xy + a_{02}y^2,$$

$$\dot{y} = x + y^2,$$

with $a_{10}, a_{01}, a_{11}, a_{02} \in \mathbf{R}$, and $a_{11} \notin \{0, 1\}$.

For convenience of further discussion, we rewrite this system as

(9)
$$\dot{x} = \lambda x + \mu y + \gamma xy + \delta(x + y^2),$$

$$\dot{y} = x + y^2,$$

with $\lambda, \mu, \gamma, \delta \in \mathbf{R}$ and $\gamma \notin \{0, 1\}$. Also, we may take $\lambda \geq 0$; if necessary, we can replace x, y and t by $x, -y$ and $-t$, respectively. In addition, without loss of generality, we can set $\lambda \in \{0, 1\}$.

The conditions on the coefficients in (1) such that a system belongs to the class studied in this section are also given in the appendix.

As a consequence of Theorem C in Coppel [**8**], the system (9) has at most one limit cycle, since the highest degree terms of P and Q are both divisible by the highest degree terms of the divergence $P_x + Q_y$, and, if this limit cycle exists, it is hyperbolic.

In summary, we have the following result:

Property 2. (i) *Quadratic systems of class $m_f = 3$ with an $M_{1,2}^i$ type of infinite critical point can be represented by* (9), *where $\mu, \gamma, \delta \in \mathbf{R}$ and $\gamma \notin \{0, 1\}$, $\lambda \in \{0, 1\}$;*

(ii) *Quadratic system* (9) *has at most one limit cycle, and, if it exists, it is hyperbolic.*

(d) $\gamma \geq 2$: elliptic saddle $M_{1,2}^1$

(c) $1 < \gamma < 2$: elliptic saddle node $M_{1,2}^1$

(b) $0 < \gamma < 1$: third order nilpotent saddle $M_{1,2}^{-1}$
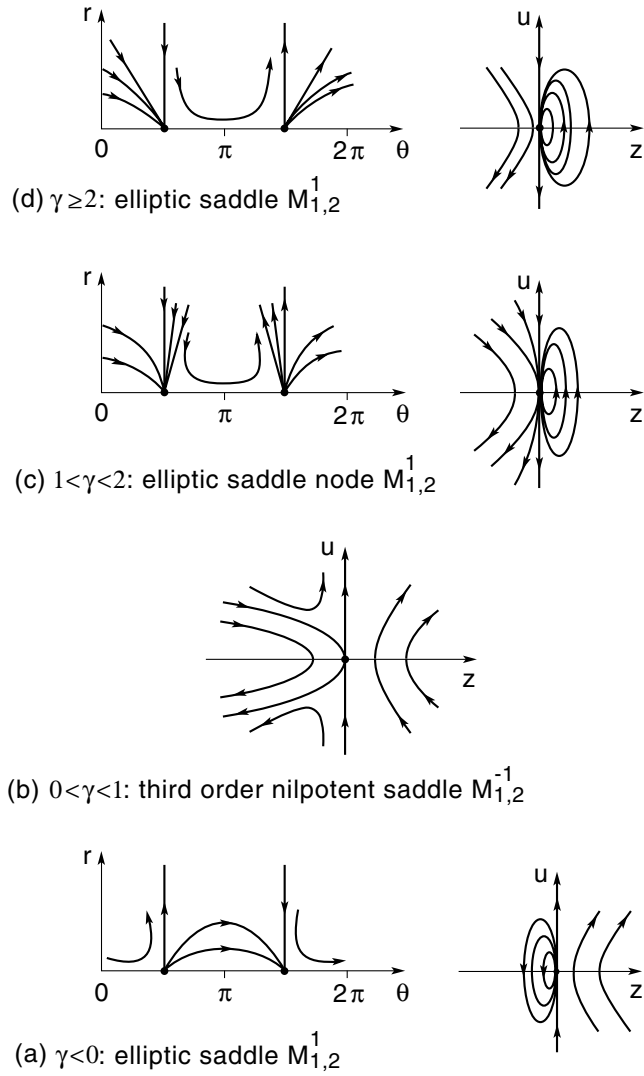

(a) $\gamma < 0$: elliptic saddle $M_{1,2}^1$

FIGURE 7. Local structure of critical point $M_{1,2}^i$ at the "ends of the x-axis" of system (9).

5. Critical points of system (9).

5.1. Critical points at infinity. We first study the critical points at infinity. By using the Poincaré transformation $z = x^{-1}$, $u = yx^{-1}$, after a scaling of time (9) becomes

$$(10) \quad \begin{aligned} z' &= -z((\lambda + \delta)z + \gamma u + \mu uz + \delta u^2) \equiv R(z, u), \\ u' &= z + (1 - \gamma)u^2 - (\lambda + \delta)zu - \mu zu^2 - \delta u^3 \equiv S(z, u), \end{aligned}$$

so if $\delta \neq 0$, the critical points at infinity are located at $z = 0$, $u = 0$ and $z = 0$, $u = (1 - \gamma)/\delta$. If $\delta = 0$, the first critical point at infinity still appears at the origin of (10), but the second one moves to 'the end of the y-axis,' which can be transformed by using another Poincaré transformation $w = y^{-1}$, $v = xy^{-1}$, into the origin of

$$(11) \quad \begin{aligned} w' &= -w(vw + 1), \\ v' &= (\gamma - 1)v + \mu w + \lambda vw - wv^2. \end{aligned}$$

In order to investigate the critical point $M_{1,2}^i$ of (10) at $(0, 0)$, we make use of the results of the analysis given in [**2**]. In order to obtain some further details, we use polar coordinates $z = r\cos\theta$, $u = r\sin\theta$, $0 \leq \theta < 2\pi$, then we get

$$(12)$$
$$\begin{aligned} r' &= r\cos\theta\sin\theta + r^2[-(\lambda + \delta)\cos^3\theta + (1 - \gamma)\sin^3\theta - \cos^2\theta\sin\theta \\ &\quad - (\lambda + \delta)\cos\theta\sin^2\theta] + r^3[-\mu\cos\theta\sin\theta - \delta\sin^2\theta], \\ \theta' &= \cos^2\theta + r\sin^2\theta\cos\theta. \end{aligned}$$

It is clear that, for $r = 0$, there are only critical points in $(0, \pi/2)$ and $(0, 3\pi/2)$. Near $(0, \pi/2)$ we write, with $\xi = \theta - \pi/2$, approximately,

$$(13) \quad \begin{aligned} r' &= -r\xi + (1 - \gamma)r^2, \\ \xi' &= -r\xi + \xi^2, \end{aligned}$$

and, similarly, near $(0, 3\pi/2)$ with $\xi = \theta - 3\pi/2$, approximately,

$$(14) \quad \begin{aligned} r' &= -r\xi - (1 - \gamma)r^2, \\ \xi' &= -r\xi + \xi^2. \end{aligned}$$

If $0 < \gamma < 1$, we may apply Theorem 66 of [**2**] with $k = 3$, $m = 1$, and it follows that $M_{1,2}^i$ is a third order nilpotent saddle $M_{1,2}^{-1}$ with

three hyperbolic sectors in $z < 0$. See Figure 7b. If $\gamma < 0$ or $\gamma > 1$, according to Theorem 66 of [**2**], the critical point $M_{1,2}^i$ is a nilpotent point with an elliptic and a hyperbolic sector. To determine the location of the separatrices of the hyperbolic sector, as compared with $z \equiv 0$, we will make use of (13) and (14). It may be seen that there are three directions $r = k\xi$ in which orbits enter the critical points $(0, \pi/2)$ and $(0, 3\pi/2)$ in the (r, θ) plane. These are $k = 0$, $k = \infty$ for both points and $k = -2/(\gamma - 2)$ for $(0, \pi/2)$ and $k = 2/(\gamma - 2)$ for $(0, 3\pi/2)$. Then, putting $\phi \equiv r - k\xi$ with fixed k, for the variation of ϕ along a solution curve of (13) can be written $\phi' = \xi^2 k[-2 + (2 - \gamma)k]$ and similarly for (14), $\phi' = \xi^2 k[-2 - (2 - \gamma)k]$. Near $r = 0$, $\theta = \pi/2$ then follows for $r > 0$, $\xi > 0$, that if $\gamma \geq 2$, $\phi' < 0$ on $k \in (0, \infty)$ which indicates that $r > 0$, $\xi > 0$ is a hyperbolic sector. Combined with a similar result near $\theta = 3\pi/2$, this shows that in the u, z plane $z \equiv 0$ is the separatrix of the hyperbolic sector in $z < 0$. The nilpotent elliptic saddle $M_{1,2}^1$ for $\gamma \geq 2$ is given in Figure 7d. For $1 < \gamma < 2$, $M_{1,2}^i$ is a nilpotent elliptic saddle node $M_{1,2}^1$ with an elliptic sector in the half plane $z > 0$ and a hyperbolic sector in the half plane $z < 0$, which also contains the separatrices. See Figure 7c. For $\gamma < 0$, $M_{1,2}^i$ is a third order nilpotent elliptic saddle $M_{1,2}^1$ with an elliptic sector in the half plane $z < 0$ and a hyperbolic sector coinciding with the half plane $z > 0$, i.e., $z \equiv 0$ coincides with the separatrices of the hyperbolic sector. See Figure 7a.

As for the other critical point at infinity, it is easy to show that it is an elementary critical point. In fact, the product of the eigenvalues of the coefficient matrix of the locally linearized system in this infinite critical point equals $\Omega(0, (1 - \gamma)/\delta) = (1/\delta^2)(1 - \gamma)^3$, where $\Omega(z, u) = (\partial R/\partial z)(z, u)(\partial S/\partial u)(z, u) - (\partial R/\partial u)(z, u)(\partial S/\partial z)(z, u)$. Hence, when $1 - \gamma < 0$, this point is a saddle, and when $1 - \gamma > 0$, a node. This result may also be obtained using (11). The character of the critical points at infinity is listed in Table 1.

5.2. Finite critical points: $\lambda = 0$. For $\lambda = 0$, system (9) reads

$$
\begin{aligned}
(15) \qquad \dot{x} &= \mu y + \gamma xy + \delta(x + y^2), \\
\dot{y} &= x + y^2,
\end{aligned}
$$

with $u, \delta, \gamma \in \mathbf{R}$, $\gamma \notin \{0, 1\}$. For this case, the critical points in the finite part of the plane are $P_0 = (x_0, y_0) = (0, 0)$, $P_+ = (x_+, y_+) = (-\mu/\gamma, \sqrt{\mu/\gamma})$, and $P_- = (x_-, y_-) = (-\mu/\gamma, -\sqrt{\mu/\gamma})$.

TABLE 1. Character of the critical points at infinity.

	$M_{1,2}^i$	Fig.	E	Σi
$\gamma < 0$	$M_{1,2}^1$ elliptic saddle	7a	node	2
$0 < \gamma < 1$	$M_{1,2}^{-1}$ saddle	7b	node	0
$1 < \gamma < 2$	$M_{1,2}^1$ elliptic saddle node	7c	saddle	0
$\gamma \geq 2$	$M_{1,2}^1$ elliptic saddle	7d	saddle	0

If $\mu\gamma < 0$, P_- and P_+ are complex leaving $P_0 = (0,0)$ to be the only real point.

If $\mu = 0$ (recall that $\gamma \neq 0$), P_0, P_- and P_+ merge into a third order critical point, which can be analyzed in a similar way as is done for the third order point at infinity, and for which the results are summarized in Figure 8.

It appears that if $\delta \neq 0$, for $\gamma < 0$, $(0,0)$ is a third order saddle and for $\gamma > 0$ a third order node both with center manifolds tangent to the y axis. For $\delta = 0$, $\gamma < 0$, $(0,0)$ is a third order saddle, for $0 < \gamma \leq 2$ an elliptic saddle and for $\gamma > 2$ and elliptic saddle node, all points being nilpotent.

If $\mu\gamma > 0$, P_0, P_- and P_+ are distinct real elementary critical points. The character of the elementary critical points may be obtained using standard arguments. For the product of the eigenvalues of the locally linearized system is found in $P_0 : \Omega = -\mu$ and in P_- and P_+: $\Omega = 2\mu$. As a result, for $\mu < 0$, P_0 is an antisaddle and P_- and P_+ are saddles or complex. In case the critical point is an antisaddle it can be a node a (weak) focus or a center. It is important to notify when such a point is a weak focus or a center. For $\mu < 0$ follows, P_0 then being an antisaddle, that for $\delta = 0$, P_0 is a center upon linearization and also for the full nonlinear system since solutions are symmetric around the x-axis. For $\delta < 0$, P_0 is stable, and for $\delta > 0$ unstable. For $\mu > 0$, $\gamma > 0$, P_- and P_+ are antisaddles and upon local linearization they are a center for $\delta_- = (\gamma + 2)\sqrt{\mu/\gamma} > 0$ and $\delta_+ = -(\gamma + 2)\sqrt{\mu/\gamma} < 0$, respectively. Upon calculating the focal values, however, they appear to be first order weak foci, being unstable and stable, respectively. Moreover, P_- is unstable for $\delta \geq \delta_-$ and stable for $\delta < \delta_-$, whereas P_+ is unstable for $\delta > \delta_+$ and stable for $\delta \leq \delta_+$. The properties of the critical points

(e) g>0, d<0;
    node m_3^1

(f) g>2, d=0;
    elliptic saddle node m_3^1

(g) g>0, d>0;
    node m_3^1

(d) 0<g $^\varepsilon$ 2, d=0;
    elliptic saddle m_3^1

(a) g<0, d<0;
    saddle m_3^{-1}

(b) g<0, d=0;
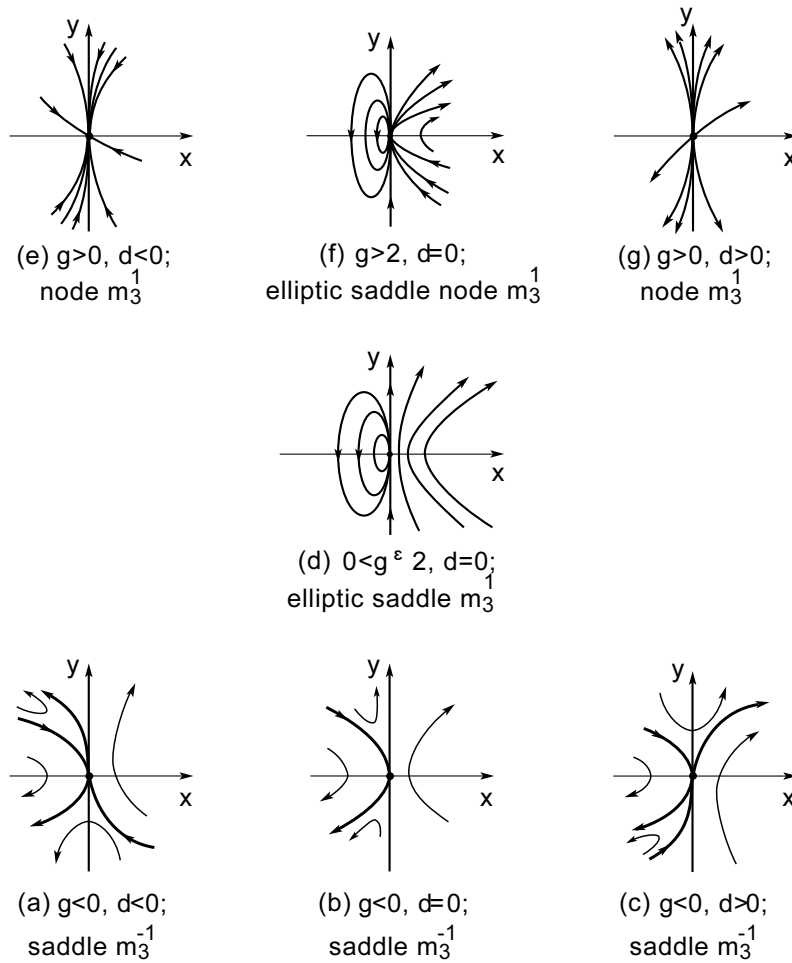   saddle m_3^{-1}

(c) g<0, d>0;
    saddle m_3^{-1}

FIGURE 8.   Local structure of the critical point in $(0,0)$ of system (9):
$\lambda = \mu = 0$.

in the finite part of the plane for $\lambda = 0$ are collected in Table 2.

5.3. Finite critical points: $\lambda = 1$. For $\lambda = 1$, system (9) reads:

$$(16) \qquad \begin{aligned} \dot{x} &= x + \mu y + \gamma xy + \delta(x + y^2), \\ \dot{y} &= x + y^2, \end{aligned}$$

with $\mu, \gamma, \delta \in \mathbf{R}$ and $\gamma \notin \{0, 1\}$.

In this case, the critical points in the finite part of the plane are $P_0 = (x_0, y_0) = (0, 0)$, $P_+ = (x_+, y_+) = ((1/(2\gamma^2))[-1 - 2\mu\gamma + \sqrt{1 + 4\mu\gamma}], (1/(2\gamma))[-1 + \sqrt{1 + 4\mu\gamma}])$, and $P_- = (x_-, y_-) = ((1/(2\gamma^2))[-1 - 2\mu\gamma - \sqrt{1 + 4\mu\gamma}, (1/(2\gamma))[-1 - \sqrt{1 + 4\mu\gamma}])$. As in the case $\lambda = 0$ but now for $1 + 4\gamma\mu < 0$, P_- and P_+ are complex critical points, leaving $P_0 = (0, 0)$ to be the only real critical point. If $1 + 4\gamma\mu = 0$ the points P_- and P_+ merge to form a second order critical point. If $1 + 4\gamma\mu > 0$, P_0, P_- and P_+ are real elementary points, except if $\mu = 0$; then P_0 and P_+ merge to form another second order critical point. The situation is indicated in Figure 9 where the parameter plane μ, γ is given. It should be remarked that not all values of μ, γ need be considered, since linear transformations can be used to transform the system into one of the same form, yet with different

TABLE 2. Finite critical points: $\lambda = 0$; $\delta_\pm = \mp(\gamma + 2)\sqrt{\mu/\gamma}$, $\delta_+ < 0 < \delta_-$.

		P_0		P_+	P_-
$\gamma < 0$	$\mu < 0$	$\delta < 0$ stable antisaddle $\delta = 0$ center $\delta > 0$ unstable antisaddle		saddle	
	$\mu = 0$	P_0, P_- and P_+ merge into a third order point; see Figure 8			
	$\mu > 0$	saddle			
$\gamma > 0$	$\mu < 0$	$\delta < 0$ stable antisaddle $\delta = 0$ center $\delta > 0$ unstable antisaddle		complex	
	$\mu = 0$	P_0, P_- and P_+ merge into a third order point; see Figure 8			
	$\mu > 0$	saddle	$\delta \leq \delta_+$	stable antisaddle	
			$\delta_+ < \delta < \delta_-$	unst. antisaddle	st. antisaddle
			$\delta \geq \delta_-$	unstable antisaddle	

values for the coefficients. In order to see this, in the μ, γ plane the following regions are distinguished:

$$
\begin{aligned}
&R_1 : \mu \geq 0, && \gamma > 0, && (\gamma \neq 1), \\
&R_2 : \mu \leq 0, && \gamma > 0, && 1 + 4\mu\gamma \geq 0, && (\gamma \neq 1), \\
&R_3 : \mu < 0, && \gamma > 0, && 1 + 4\mu\gamma < 0 && (\gamma \neq 1), \\
&R_4 : \mu \leq 0, && \gamma < 0, \\
&R_5 : \mu \geq 0, && \gamma < 0, && 1 + 4\mu\gamma \geq 0, \\
&R_6 : \mu > 0, && \gamma < 0, && 1 + 4\mu\gamma < 0.
\end{aligned}
$$

Now from Table 1 it follows that the sum of the indices of the critical points at infinity equals 0 for $\gamma > 0$ and 2 for $\gamma < 0$. From it follows that the sum of the indices of the finite critical points equals 1 for $\gamma > 0$ and -1 for $\gamma < 0$. As a result, regions in $\gamma > 0$ and $\gamma < 0$ cannot be mapped onto each other. Also, neither region R_1 nor R_2 (R_4 nor R_5) can be mapped onto $R_3(R_6)$, since only the latter contains complex critical points. However, $R_1(R_4)$ and $R_2(R_5)$ can be mapped onto each other as follows. Consider a point in R_2 and shift P_+ to the origin of a new coordinate system (x_1, y_1) by the shift $x = x_1 + x_+, \ y = y_1 + y_+$ and apply further the transformation $x_2 = x_1 + 2y_+y_1, y_2 = y_1$, then (16) becomes, using again the notation x, y instead of x_2, y_2,

$$
\begin{aligned}
\dot{x} &= \lambda_1 x + \mu_1 y + \gamma xy + \delta_1(x + y^2), \\
\dot{y} &= x + y^2,
\end{aligned}
\tag{17}
$$

where $\lambda_1 = 1 + 3\gamma y_+, \mu_1 = y_+ - 2\mu = (1/(2\gamma))(1 - \sqrt{1 + 4\mu\gamma})\sqrt{1 + 4\mu\gamma} \geq 0$ and $\delta_1 = \delta + 2(1 - \gamma)y_+$. Now if $\mu\gamma = -2/9$, there follows $\lambda_1 = 0$, and we may refer to the previous Section 5.2. If $\lambda_1 \neq 0$, replace x by $\lambda_1^2 x$, y by $\lambda_1 y$ and t by $(1/\lambda_1)t$, then (17) becomes

$$
\begin{aligned}
\dot{x} &= x + \mu_2 y + \gamma xy + \delta_2(x + y^2), \\
\dot{y} &= x + y^2,
\end{aligned}
\tag{18}
$$

where $\mu_2 = \mu_1/\lambda_1^2$, $\delta_2 = \delta_1/\lambda_1$, and R_1 and R_2 are mapped onto each other. Similarly, this can be shown for R_4 and R_5. As a result, we may restrict our attention to the regions R_1, R_3, R_4 and R_6 in the parameter space $(\mu, \gamma.\delta)$.

For the character of the elementary critical points, we consider the product of the eigenvalues of the coefficient matrix of the locally
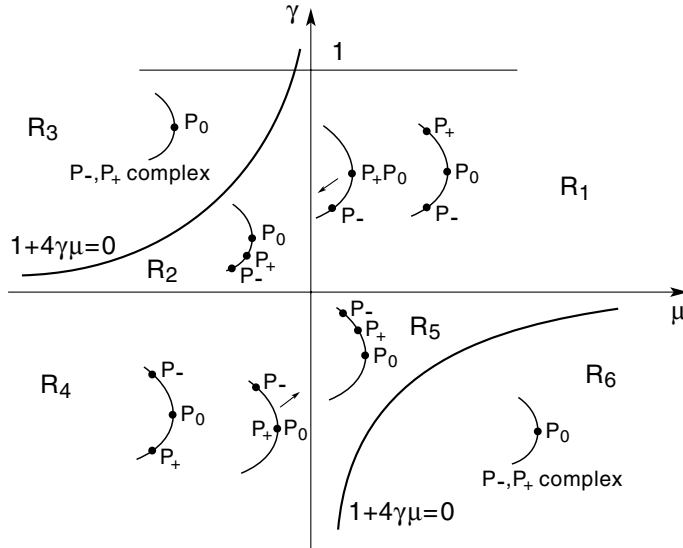
FIGURE 9. Location of the finite critical points for the various regions in parameter plane μ, γ.

linearized system $\Omega(0,0) = -\mu$. Thus, for $\mu < 0$, the origin P_0 is an antisaddle and, since for $\gamma < 0$ the sum of the indices of the finite critical points equals -1, the points P_- and P_+ are both saddles whereas for $\gamma > 0$ they are complex if $1 + 4\mu\gamma < 0$. For $\mu > 0$, P_0 is a saddle and since, for $\gamma > 0$, the sum of the indices of the finite critical points equals $+1$, the points P_- and P_+ are both antisaddles, whereas for $\gamma < 0$ they are complex if $1 + 4\mu\gamma < 0$. If the elementary critical points are antisaddles, calculation of the focal values in case they are weak foci yields whether they are centers, first order weak foci and what their stability is. Mergence of elementary critical points into second order critical points at $\mu = 0$ or $1 + 4\mu\gamma = 0$ can be studied using the classification in [**2**]. The properties of the critical points in the finite part of the plane for $\lambda = 1$ are collected in Table 3.

5.4. Conclusions. In summary, Section 5 leads to the following result:

Property 3. (i) *System* (9) *has a nilpotent third order critical point*

TABLE 3. Finite critical points: $\lambda = 1$, $\delta_\pm = (1/(2\gamma))[-\gamma + 2 \mp (\gamma + 2)\sqrt{1+4\mu\gamma}]$, $\delta_+ < 0 < \delta_-$.

			P_0	P_+	P_-
$\gamma<0$	$\mu<0$	$\delta<-1$	stable antisaddle	saddle	
		$\delta=-1$	$\gamma<-2$, unst. 1 weak focus; $\gamma=-2$, center; $-2<\gamma<0$, st. 1 w. focus		
		$\delta>-1$	unstable antisaddle		
	$\mu=0$	$\delta<-1$	P_0, P_+ merge into a 2nd order saddle node, eigen val. <0		
		$\delta=-1$	P_0, P_+ merge into a 2nd order cusp		
		$\delta>-1$	P_0, P_+ merge into a 2nd order saddle node, eigen val. >0		
	$\mu>0$	$1+4\mu\gamma<0$	saddle	complex	
$\gamma>0$	$\mu<0$	$1+4\mu\gamma<0$; $\delta<-1$	stable antisaddle	complex	$\delta<\delta_-$, stable antisaddle
		$\delta=-1$	stable 1 weak focus		$\delta\geq\delta_-$, unstable antisaddle
		$\delta>-1$	unstable antisaddle		
	$\mu=0$	$\delta<-1$	P_0, P_+ merge into a 2nd order saddle node, eigen val. <0		
		$\delta=-1$	P_0, P_+ merge into a 2nd order cusp		
		$\delta>-1$	P_0, P_+ merge into a 2nd order saddle node, eigen val. >0		
	$\mu>0$		saddle	$\delta\leq\delta_+$, stable antisaddle; $\delta>\delta_+$, unstable antisaddle	

at the ends of the x axis; it is either an elliptic saddle (saddle node) $M_{1,2}^1$ or a saddle $M_{1,2}^{-1}$, and its local structure is given in Figure 7. The other critical point at infinity is elementary and either a saddle or a node. The character of the critical points at infinity is listed in Table 1.

(ii) *System (9) has three finite critical points, possibly pairwise complex or coinciding in a second order ($\lambda = 1$) or third order critical point ($\lambda = 0$). For $\lambda = 0$ these points are listed in Table 2 and the third order point is illustrated in Figure 8. For $\lambda = 1$, they are given in Table 3.*

(iii) *The phase portraits of system (9) can be determined by considering the parameter values in the following regions: $R_1 : \mu \geq 0$, $\gamma > 0$ ($\gamma \neq 1$), $R_3 : \mu < 0$, $\gamma > 0$ ($\gamma \neq 0$), $1 + 4\mu\gamma < 0$, $R_4 : \mu \leq 0$, $\gamma < 0$ and $R_6 : \mu > 0$, $\gamma < 0$, $1 + 4\mu\gamma < 0$, whereas $\delta \in \mathbf{R}$.*

6. Phase portraits of system (9): $\lambda = 0$. Recall that system (9) reads

(19)
$$\begin{aligned} \dot{x} &= \lambda x + \mu y + \gamma xy + \delta(x + y^2) \equiv P(x, y), \\ \dot{y} &= x + y^2 \equiv Q(x, y), \end{aligned}$$

where $\lambda, \mu, \gamma, \delta \in \mathbf{R}$, $\gamma \notin \{0, 1\}$.

The phase portraits of (9) will be studied using standard arguments in the theory of quadratic systems and the known properties of (9), as listed in the previous section. One of the reasons that the class of systems to be studied is represented in the form given by (9) is that now δ is a parameter rotating the field. This may be seen by calculating

$$PQ_\delta - QP_\delta = -(x + y^2)^2,$$

which is negative outside the parabola $x + y^2 = 0$. This fact will be used in the search for bifurcation phenomena in parameter space. Since the parameter space is $\mathbf{R}^4$, the ordering of the phase portraits in this space is difficult to visualize. If possible, it helps to use scaling of the variables in order to restrict the values of certain parameters to 0 or 1. This was done, for example, in the previous section, when the character of the critical points was investigated restricting the values of λ to 0 and 1. For $\lambda = 0$ this procedure can be continued and leads to the restriction $\mu = \{-1, 0, 1\}$, and so on for $\mu = 0$. A disadvantage of this procedure is that a better view on the relation between the phase portraits for a
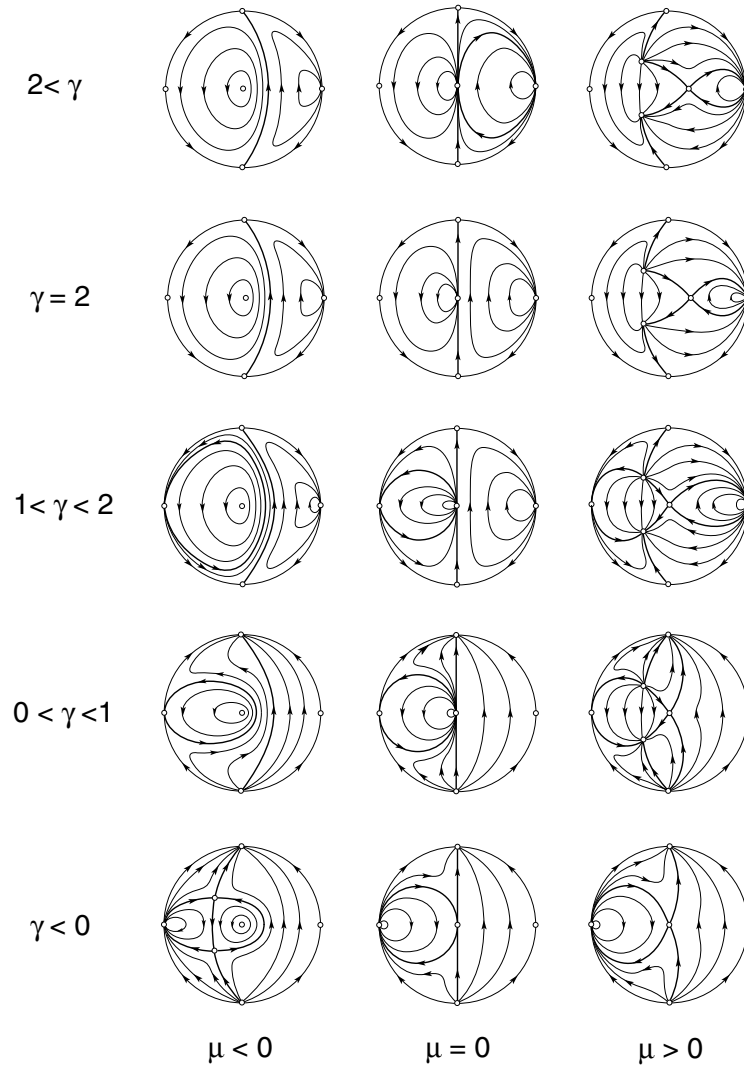
FIGURE 10.1. Phase portraits of system (9) with $\lambda = \delta = 0$.
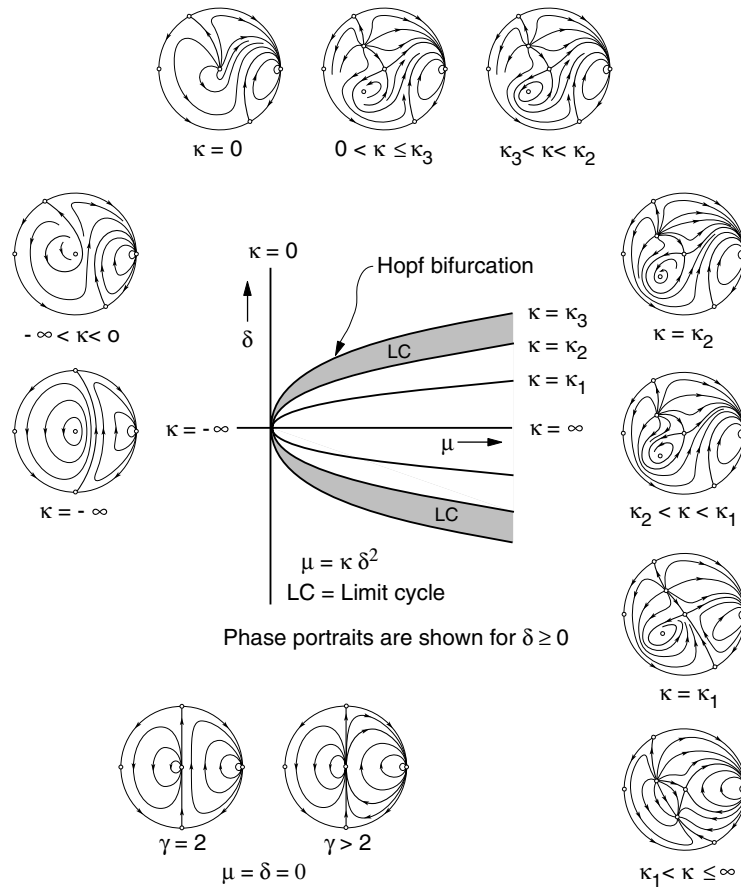
FIGURE 10.2. Bifurcation diagram and phase portraits of system (9): $\lambda = 0$, $\gamma \geq 2$.

discrete set of values of certain parameters goes at the cost of losing the information obtainable when these parameters are allowed to vary continuously. Bifurcation phenomena are then less explicitly showed. In the following, we intend to find a balance between trying to lower the number of parameters and showing the bifurcation phenomena as much as possible.
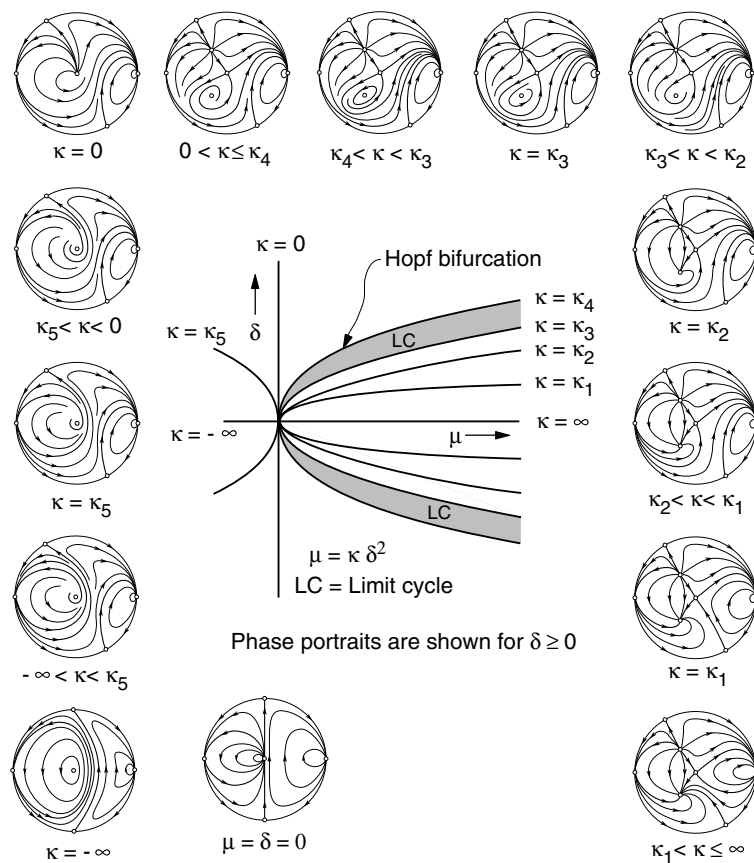
FIGURE 10.3. Bifurcation diagram and phase portraits of system (9): $\lambda = 0$, $1 < \gamma < 2$.

6.1. Phase portraits of system (9) for $\lambda = 0$, $\delta = 0$. For this case (9) reads

$$(20) \qquad \begin{aligned} \dot{x} &= \mu y + \gamma xy, \\ \dot{y} &= x + y^2, \end{aligned}$$

where $\mu, \gamma \in \mathbf{R}$, $\gamma \notin \{0, 1\}$. This system may easily be analyzed; it may in fact be integrated as a linear differential equation in y^2 and the solution curves are symmetric about the x-axis. There is one integral
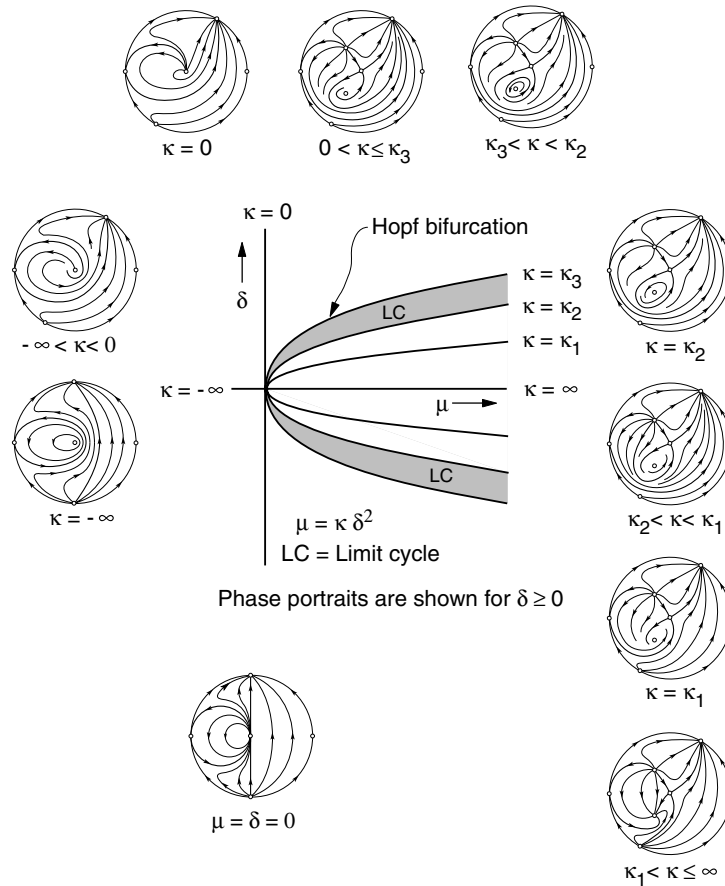
FIGURE 10.4. Bifurcation diagram and phase portraits of system (9): $\lambda = 0$, $0 < \gamma < 1$.

straight line, which is given by $x \equiv -\mu\gamma^{-1}$, whereas the infinite critical points are situated at the ends of the x and y axes. From the properties of the critical points the phase portraits can readily be constructed and are shown in Figure 10.1. Bifurcations take place at $\mu = 0$, $\gamma = 0, 1$ or 2 in the μ, γ parameter plane.

6.2. Phase portraits of system (9) for $\lambda = 0$, $\delta \neq 0$: $\gamma \geq 2$. For $\delta \neq 0$ we will break up the γ axis into several intervals and consider

what happens in each interval as a function of the remaining parameters μ and δ. This makes it more difficult to follow the bifurcations resulting from changes in γ. As pointed out before, we could also restrict ourselves to the values of μ in the set $\{-1, 0, 1\}$; however, we will keep μ as a running parameter. The possibility of using linear transformations to simplify the presentation can, however, be applied to obtain information on the structure of the bifurcation curves in the μ, δ plane. First of all, it can easily be seen, by replacing in (9) x by $-x$, y by $-y$ and t by $-t$, that the coefficient δ changes into $-\delta$ showing the symmetry around the μ axis of curves and regions of the same phase portraits. Moreover, it can, in fact, be shown that $\kappa = \mu \delta^{-2}$, $-\infty < \kappa < \infty$, is the governing parameter in the μ, δ plane since replacing x by $\delta^2 x$, y by δy, t by $\delta^{-1} t$ transforms (9) into

$$(21) \qquad \begin{aligned} \dot{x} &= (\mu/\delta^2)y + \gamma xy + x + y^2, \\ \dot{y} &= x + y^2, \end{aligned}$$

so that, for fixed γ the phase portraits on $\mu = \kappa \delta^2$ are affine equivalent for fixed κ.

The phase portraits and the bifurcation diagram in the μ, δ plane for $\gamma \geq 2$ are shown in Figure 10.2. Only the phase portraits for $\delta \geq 0$ are shown; those for $\delta < 0$ may be obtained through reflection around the x axis and time reversal. For $\mu < 0$, $\delta > 0$, the phase portrait may be obtained from that for $\delta = 0$ by considering how the vector field rotates as a result of increasing δ. For $\mu = 0$, increasing δ from $\delta = 0$ makes the elliptic saddle for $\gamma = 2$ and the elliptic saddle node for $\gamma > 2$ change into an unstable third order node; the phase portrait may further be constructed using the rotation of the vector field. For $\mu > 0$ the phase portrait for $\delta = 0$ persists over some interval of $\kappa^{-1} = \delta^2 \mu^{-1} \geq 0$ until for some value $\kappa = \kappa_1$ a connection between the finite and infinite saddle occurs, which upon increasing δ breaks in the direction given by the rotation of the vector field. This leads to the phase portrait for $\kappa_2 < \kappa < \kappa_1$. At $\kappa = \kappa_2$, a homoclinic loop occurs, for $\delta > 0$ unstable from the inside since $\operatorname{div}\{P(0,0), Q(0,0)\} = \delta$. It bifurcates a unique unstable limit cycle upon increasing δ, which contracts into P_- for $\kappa = \kappa_3 = \gamma/(\gamma + 2)^2$ as a Hopf bifurcation leading to a phase portrait which persists for $0 < \kappa \leq \kappa_3$. It is possible to determine the functions $\kappa_1 = \kappa_1(\gamma)$ and $\kappa_2 = \kappa_2(\gamma)$ numerically; it would be interesting to determine them analytically from a global bifurcation analysis of (9) for $\lambda = 0$, taking μ and δ as bifurcation parameters.
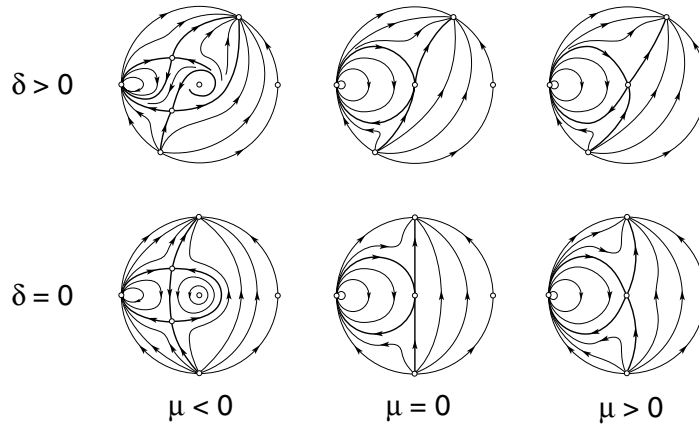
FIGURE 10.5. Bifurcation diagram and phase portraits of system (9): $\lambda = 0$, $\gamma < 0$.

6.3. Phase portraits of system (9) for $\lambda = 0$, $\delta \neq 0$: $1 < \gamma < 2$.
The phase portraits and the bifurcation diagram in the μ, δ plane for $1 < \gamma < 2$ are shown in Figure 10.3. The same arguments and similar conclusions may be obtained as in the previous Section 6.2. It appears that there are more connections possible between the finite saddle and points at infinity than in the previous case. Note that the Hopf bifurcation value is again $\gamma/(\gamma + 2)^2 (= K_4)$.

6.4. Phase portraits of system (9) for $\lambda = 0$, $\delta \neq 0$: $0 < \gamma < 1$.
The phase portraits and the bifurcation diagram in the μ, δ plane for $0 < \gamma < 1$ are shown in Figure 10.4. The same arguments and similar conclusions may be obtained as before. Also, $K_3 = \gamma/(\gamma + 2)^2$.

6.5. Phase portraits of system for $\lambda = 0$, $\delta \neq 0$: $\gamma < 0$. The phase portraits and the bifurcation diagram in the μ, δ plane for $\gamma < 0$ are shown in Figure 10.5. The same arguments and similar conclusions may be obtained as before.
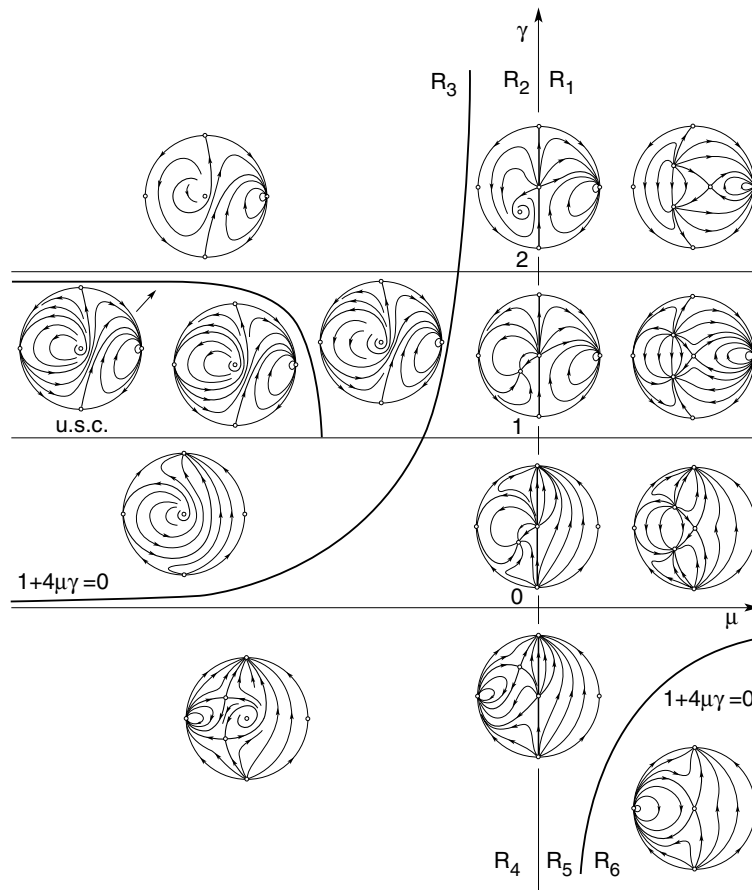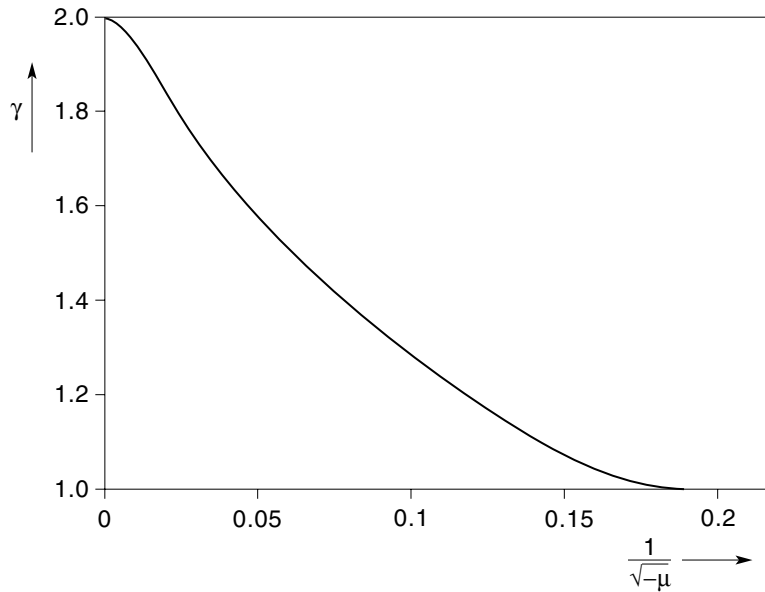
FIGURE 11.1. Bifurcation diagram and phase portraits of system (9): $\lambda = 1$, $\delta = 0$.

6.6. Conclusion.

Property 4. *A classification of the phase portraits of system* (9) *for $\lambda = 0$ leads to the 39 topologically different phase portraits given in Figure* 10.1–10.5*; they are related to the cases $\delta = 0$ and $\delta \neq 0$, $2 \leq \gamma$, $1 < \gamma < 2$, $0 < \gamma < 1$, $\gamma < 0$, respectively.*

7. Phase portraits of system (9): $\lambda = 1$. It was stated in the

FIGURE 11.1a The unbounded separatrix cycle for $\lambda = 1$, $\delta = 0$.

previous section that for $\lambda = 0$ bifurcation curves in the μ, δ plane for fixed γ can be represented by $\mu = k\delta^2$, where κ might possibly be determined from a global bifurcation analysis, taking μ and δ as bifurcation parameters. As long as this analysis is not done, numerical calculation of these curves remains an alternative to be used. As appears from the results in the rest of this section, bifurcation surfaces in the μ, δ, λ space are more complicated than for $\lambda = 0$ and more numerical calculations are needed to construct the intersections of these surfaces with the plane $\lambda \equiv 1$.

7.1. Phase portraits of system (9) for $\lambda = 1$, $\delta = 0$. These phase portraits are given in Figure 11.1. As pointed out in Section 5.3, only those in region R_1, R_3, R_4 and R_6 need be considered. The phase portraits for $\mu > 0$, $\gamma > 0$ ($\neq 1$) are topologically the same as those for $\lambda = 0$, $\delta = 0$ in the corresponding region of the μ, γ plane as are given in Figure 10.1. This can be seen by observing that these phase portraits are structurally stable with respect to small changes in λ, and λ may be scaled to 1. For $\mu = 0$, $\gamma > 0$, the critical points
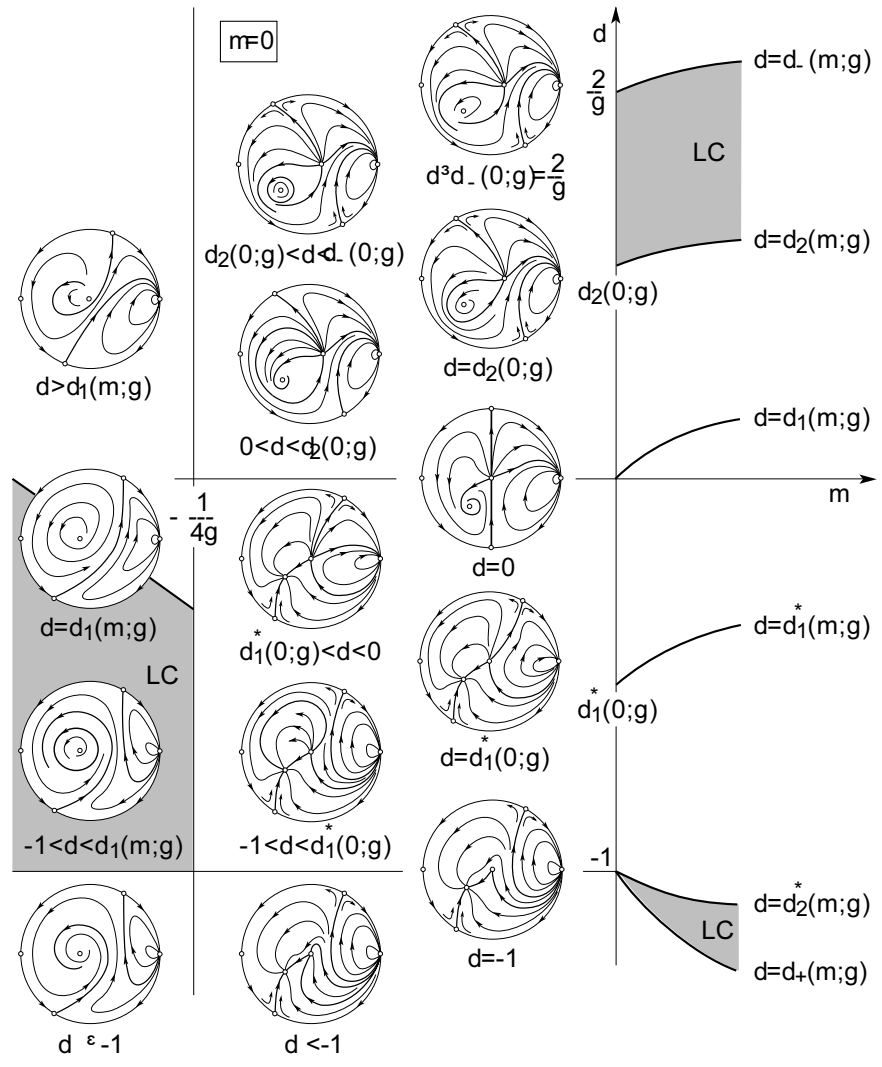
FIGURE 11.2. Bifurcation diagram and phase portraits of system (9): $\lambda = 1$, $\delta \neq 0$, $\gamma \geq 2$.
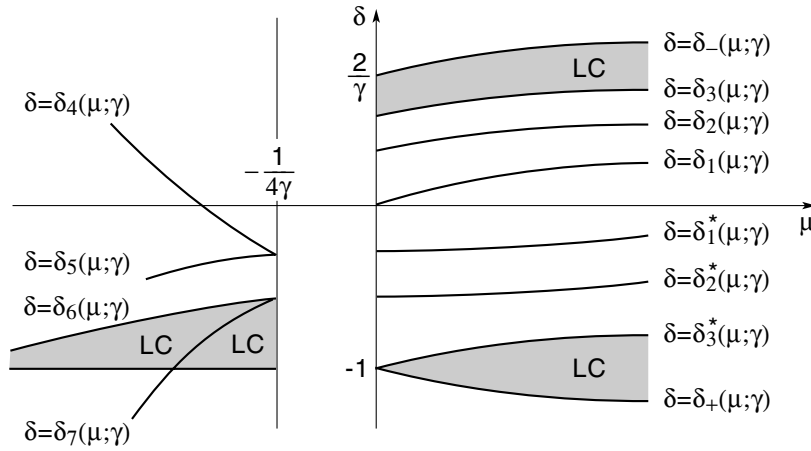
FIGURE 11.3a. Qualitative bifurcation diagram.

P_+ and P_0 coincide to form a second order saddle node in the origin, leaving a stable antisaddle in the critical point P_-. Since, moreover, $x \equiv 0$ is an invariant line, the phase portraits for $\mu = 0$ and $\gamma > 0$ are now readily determined. In region R_3 the phase portraits may be derived starting from the known properties of the critical points given in Section 5. Considering the flow across the y axis leads to the phase portrait for $\gamma \geq 2$. For $1 < \gamma < 2$ numerical evidence shows that all three separatrix structures allowed by the properties of the critical points are realized. The values of μ and γ for which the unbounded separatrix cycle occurs are given in Figure 11.1a. The phase portrait for $0 < \gamma < 1$ may directly be determined from the properties of the critical points. The phase portraits for $\mu < 0$, $\gamma < 0$ (region R_4) follow directly from the properties of the critical points. The phase portrait for $\mu = 0$, $\gamma < 0$ may be derived using similar arguments as for $\mu = 0$, $\gamma > 0$. In region R_6 the phase portrait is as for $\mu > 0$, $\gamma < 0$ in Figure 10.1, this being structurally stable under small changes of λ. (Note that the curve $1 + 4\mu\gamma = 0$ is the intersection curve with $\lambda = 1$ of the bifurcation surface $\lambda + 4\mu\gamma = 0$, which intersects the plane $\lambda = 0$ along the coordinate axes.) There are no limit cycles.
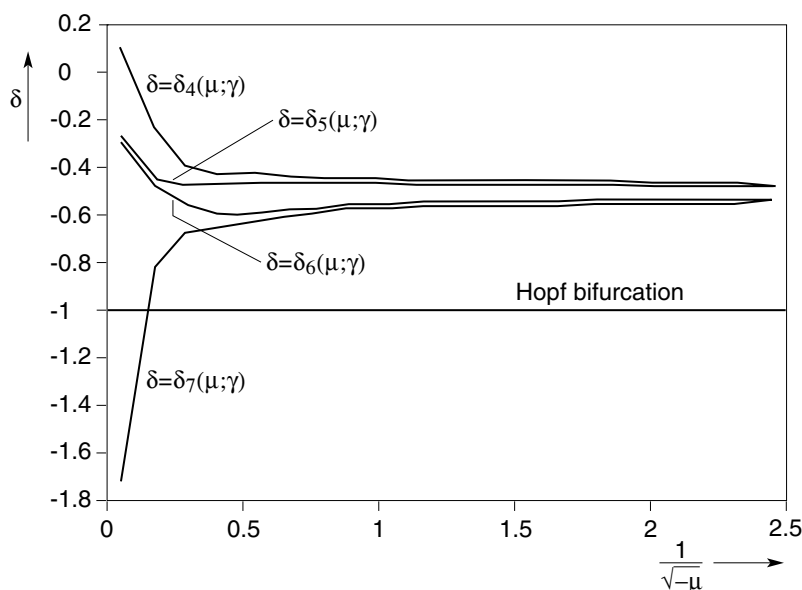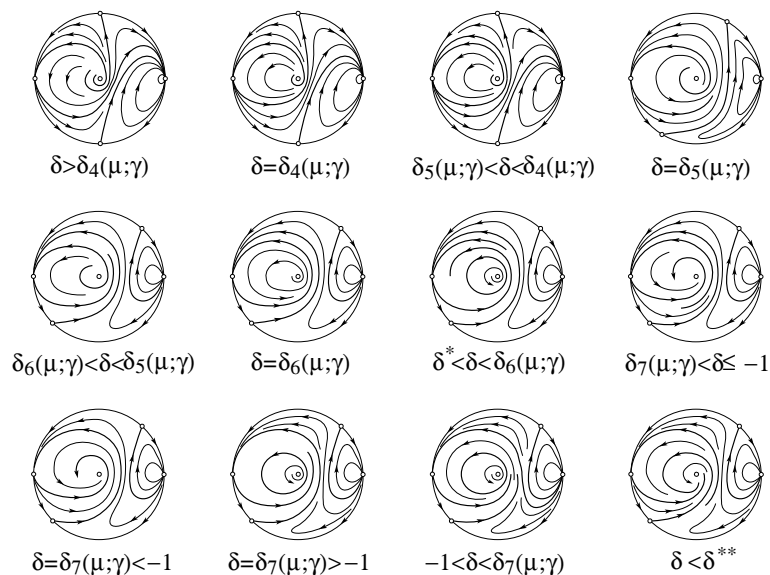
FIGURE 11.3b. Numerical results for $\mu < -1/(4\gamma)$; $\gamma = 1.5$.

7.2. Phase portraits of system (9) for $\lambda = 1$, $\delta \neq 0$: $\gamma \geq 2$.
These portraits are given in Figure 11.2. Region $\mu < -(1/(4\gamma))$
corresponds to region R_3 in the μ, γ plane. For $\mu < -1/(4\gamma)$, $\delta = 0$,
the phase portrait is as given for $\gamma \geq 2$ in Figure 11.1 and, as follows
from the direction in which the vector field is rotating, the phase
portrait remains topologically the same if δ is made positive. If δ
is made negative, the vector field rotates such that for some value of
$\delta = \delta_1(\mu; \gamma)$ an unbounded sepratrix cycle is formed, which generates a
unique stable limit cycle if δ is decreased further. Subsequent decrease
of δ makes the limit cycle shrink into a first order weak focus for $\delta = -1$,
whereas the phase portrait for this value of δ prevails for $\delta < -1$. No
numerical calculations were made to determine $\delta = \delta_1(\mu; \gamma)$. The region
$-1/(4\gamma) \leq \mu < 0$ corresponds to the region R_2 in the μ, γ plane, and
we do need to consider it.

For $\mu = 0$, $\delta = 0$, the phase portrait is given in Figure 11.1 ($\gamma \geq 2$).
Increasing δ makes the vector field rotate in clockwise direction. As
a result, first the separatrix connecting the saddle at infinity with the
saddle node in the origin is broken, whereas, subsequently, a saddle

$$\delta > \delta_4(\mu;\gamma) \qquad \delta = \delta_4(\mu;\gamma) \qquad \delta_5(\mu;\gamma) < \delta < \delta_4(\mu;\gamma) \qquad \delta = \delta_5(\mu;\gamma)$$

$$\delta_6(\mu;\gamma) < \delta < \delta_5(\mu;\gamma) \qquad \delta = \delta_6(\mu;\gamma) \qquad \delta^* < \delta < \delta_6(\mu;\gamma) \qquad \delta_7(\mu;\gamma) < \delta \leq -1$$

$$\delta = \delta_7(\mu;\gamma) < -1 \qquad \delta = \delta_7(\mu;\gamma) > -1 \qquad -1 < \delta < \delta_7(\mu;\gamma) \qquad \delta < \delta^{**}$$

$$\delta^* = \max\left(-1, \delta_7(\mu;\gamma)\right), \ \delta^{**} = \min\left(-1, \delta_7(\mu;\gamma)\right)$$

FIGURE 11.3c. Phase portraits for $\mu < -1/(4\gamma)$.

node loop is formed surrounding P_-. Upon further increase of δ, an unstable limit cycle is bifurcated which for $\delta = 2/\gamma$ disappears through a Hopf bifurcation in P_-, which is then an unstable first order weak focus. Further increase of δ does not change the topological character of the phase portrait. For all values $\delta \geq 0$ the origin is a second order saddle node with one positive eigenvalue. If δ is made negative the separatrix connecting the saddle at infinity with the saddle node in the origin breaks in the opposite direction leading to a separatrix structure shown in Figure 11.2 for $\delta_1^*(0;\gamma) < \delta < 0$. Further decrease of δ leads to the separatrix structures as shown for $-1 < \delta \leq \delta_1^*(0;\gamma)$, and the origin is still a second order saddle node with one positive eigenvalue. For $\delta = -1$ the origin is a second order cusp, and for $\delta < -1$ a second order saddle node with one negative eigenvalue.

For $\mu > 0$, $\delta = 0$ the phase portrait is as in Figure 11.1 ($\gamma \geq 2$) and also as in Figure 10.2 ($\gamma \geq 2$, $K = \infty$) and, in fact, the
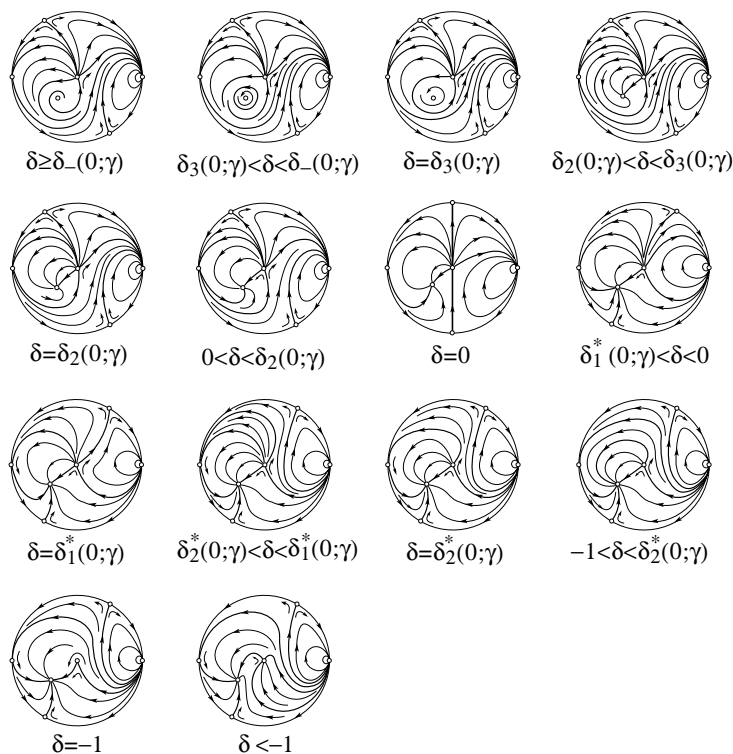
$$\delta \geq \delta_-(0;\gamma) \qquad \delta_3(0;\gamma)<\delta<\delta_-(0;\gamma) \qquad \delta=\delta_3(0;\gamma) \qquad \delta_2(0;\gamma)<\delta<\delta_3(0;\gamma)$$

$$\delta=\delta_2(0;\gamma) \qquad 0<\delta<\delta_2(0;\gamma) \qquad \delta=0 \qquad \delta_1^*(0;\gamma)<\delta<0$$

$$\delta=\delta_1^*(0;\gamma) \qquad \delta_2^*(0;\gamma)<\delta<\delta_1^*(0;\gamma) \qquad \delta=\delta_2^*(0;\gamma) \qquad -1<\delta<\delta_2^*(0;\gamma)$$

$$\delta=-1 \qquad \delta<-1$$

FIGURE 11.3d. Phase portraits for $\mu=0$.

bifurcation diagram and phase portraits of Figures 10.2 and 11.2 are qualitatively the same for $\mu>0$. It should be noted, however, that in Figure 10.2 only the phase portraits for $\delta \geq 0$ are shown, and limit cycle formation takes place around P_-. In Figure 11.2 the same occurs for $\delta \geq 0$, the critical point P_- being a first order unstable weak focus for $\delta=\delta_-=(1/(2\gamma))[2-\gamma+(2+\gamma)\sqrt{1+4\mu\gamma}]$. For $\delta<0$ the phase portraits are topologically equivalent to that for $\delta>0$; the limit cycle formation now taking place around P_+, which is a first order stable weak focus for $\delta=\delta_+=(1/(2\gamma))[2-\gamma-(2+\gamma)\sqrt{1+4\mu\gamma}]$.

7.3. Phase portraits of system (9) for $\lambda=1$, $\delta \neq 0$: $1<\gamma<2$. These phase portraits are given in Figure 11.3. As when going from Figure 10.2 to Figure 10.3, the bifurcation diagram becomes more
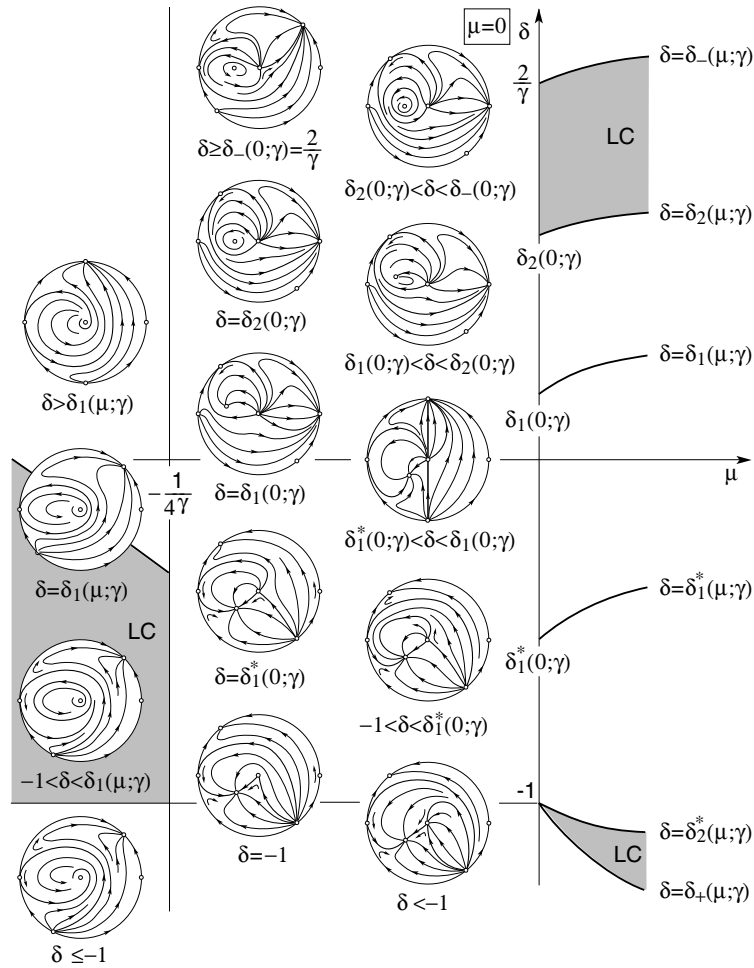
FIGURE 11.4. Bifurcation diagram and phase portraits of system (9) for $\lambda = 1$, $\delta \neq 0$; $0 < \gamma < 1$.

complicated and more phase portraits occur as a result of the presence of two more separatrices from the critical point $M_{1,2}^1$ at infinity. For $\mu \geq 0$ the same remarks apply as for the case $\gamma \geq 2$, including the expressions for δ_- and δ_+. No numerical calculations of bifurcation curves for $\mu > 0$ were made because the qualitative structure of the
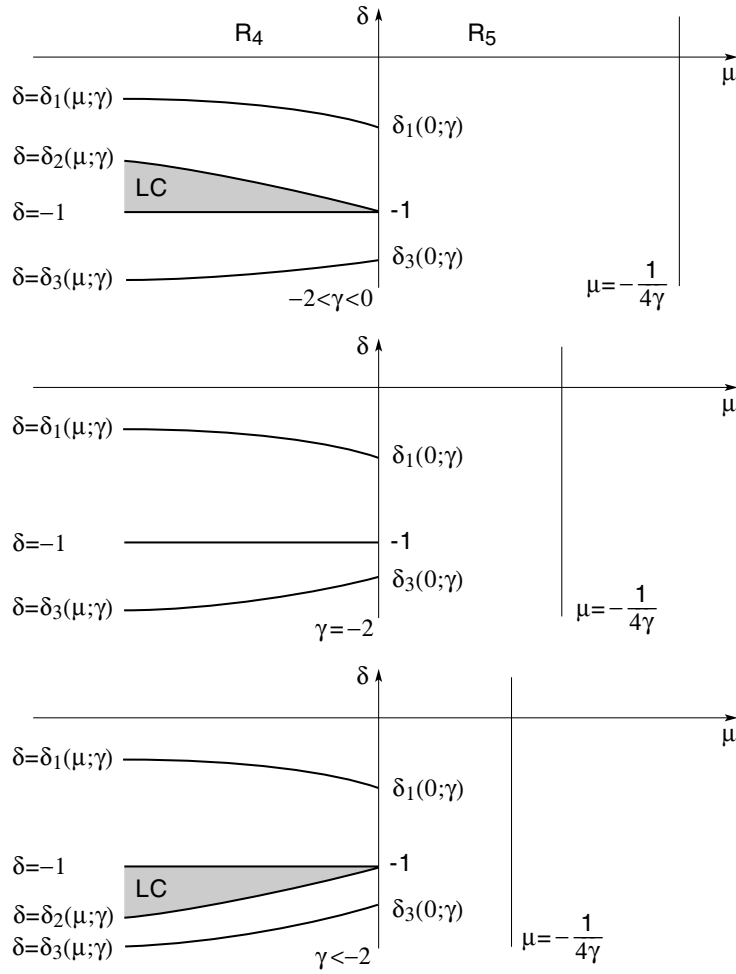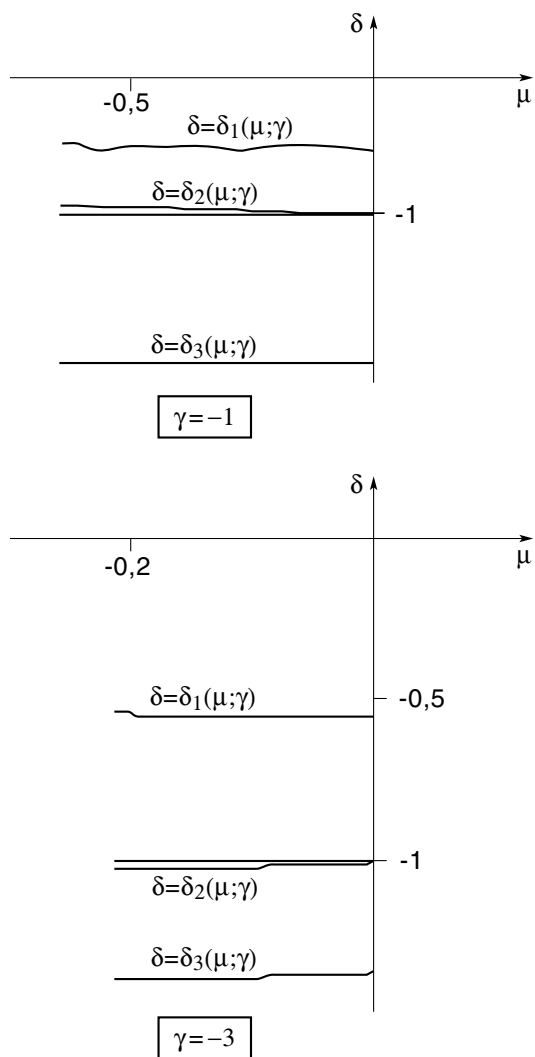
FIGURE 11.5a. Qualitative bifurcation diagrams.

FIGURE 11.5b. Numerical results for the bifurcation curves for $\mu < 0$.

$\delta > \delta_1(\mu;\gamma)$ $\delta = \delta_1(\mu;\gamma)$ $\delta_2(\mu;\gamma) < \delta < \delta_1(\mu;\gamma)$ $\delta = \delta_2(\mu;\gamma)$

$-1 < \delta < \delta_2(\mu;\gamma)$ $\delta_3(\mu;\gamma) < \delta \leq -1$ $\delta = \delta_3(\mu;\gamma)$ $\delta > \delta_3(\mu;\gamma)$

$\mu < 0,\ -2 < \gamma < 0$

$\delta = -1$ $\delta_2(\mu;\gamma) < \delta < -1$ $\delta = \delta_2(\mu;\gamma)$

$\mu < 0,\ \gamma = -2$ $\mu < 0,\ \gamma > -2$

$\delta > \delta_1(0;\gamma)$ $\delta = \delta_1(0;\gamma)$ $-1 < \delta < \delta_1(0;\gamma)$ $\delta = -1$

$\delta_3(0;\gamma) < \delta < -1$ $\delta = \delta_3(0;\gamma)$ $\delta > \delta_3(0;\gamma)$

$\mu = 0,\ \gamma < 0$
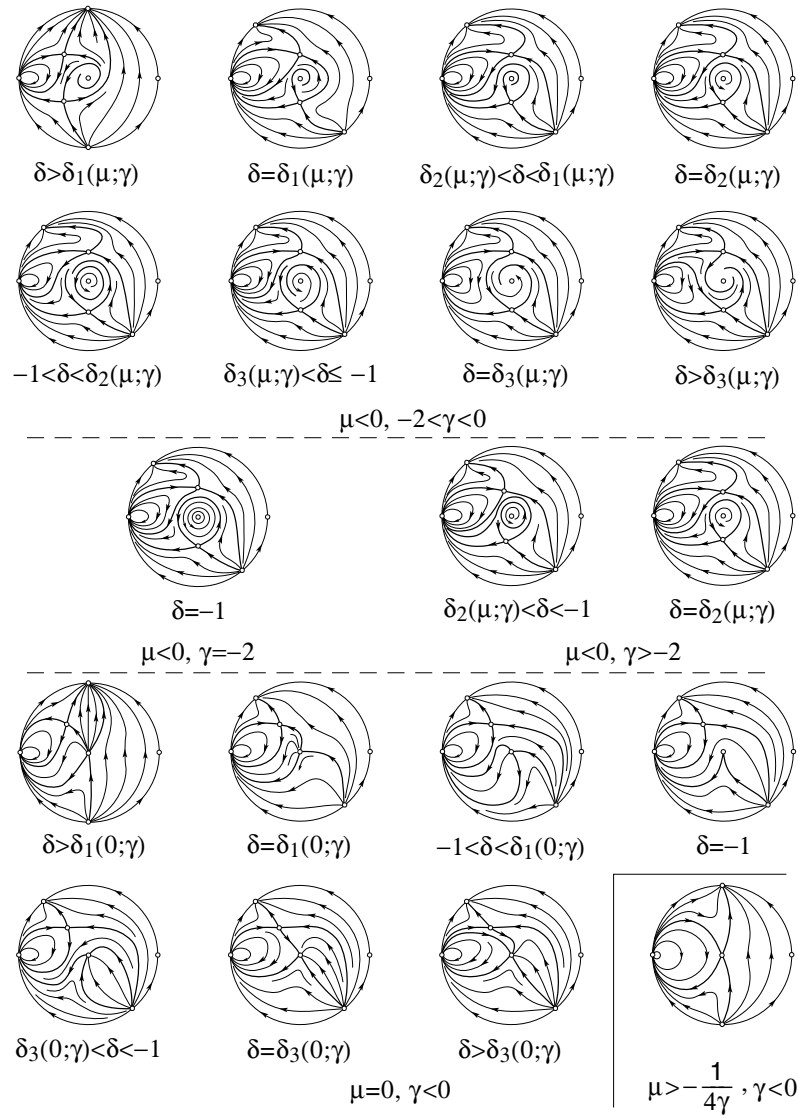
$\mu > -\dfrac{1}{4\gamma},\ \gamma < 0$

FIGURE 11.5c. Phase portraits.

bifurcation diagram is clear.

For $\mu < -1/(4\gamma)$ there exists but one finite critical point. In order to find the separatrix structure, numerical calculations are needed, and bifurcation curves obtained in this way are given in Figure 11.3b.

7.4. Phase portraits of system (9) for $\lambda = 1$, $\delta \neq 0$: $0 < \gamma < 1$. These phase portraits are given in Figure 11.4. Bifurcation diagram and phase portraits should be compared with those of Figure 10.4. Since no new arguments are used, no further explanation is given.

7.5. Phase portraits of system (9) for $\lambda = 1$, $\delta \neq 0$: $\gamma < 0$. These phase portraits are given in Figure 11.5. As appears from Table 3, apart from weak foci of the first order, also a centerpoint can occur. In fact, for $\mu < 0$, $\delta = -1$, the origin (P_0) is a first order weak focus if $\gamma \neq -2$ and a centerpoint if $\gamma = -2$. This may be seen by replacing x by $-\mu x$, y by $\sqrt{-\mu}y$ and t by $(1/\sqrt{-\mu})t$, then (11) becomes, with $\delta = -1$:

$$\text{(22)} \qquad \dot{x} = -y + \gamma xy - \frac{1}{\sqrt{-\mu}}y^2,$$
$$\dot{y} = x + y^2.$$

The result follows by noting that the first focal value $W_1 = -(\gamma + 2)/\sqrt{-\mu} \neq 0$ for $\gamma \neq -2$, whereas for $\gamma = -2$ it follows that $W_1 = W_2 = W_3 = 0$ [**21**].

The numerical calculations confirm the qualitative behavior of the bifurcation diagrams and also show that the limit cycle occurs in a very tiny δ interval.

7.6. Conclusion.

Property 5. *A classification of phase portraits of system* (9) *for $\lambda = 1$ leads to* 80 *topologically different phase portraits not yet contained in the classification for $\lambda = 0$. They are given in Figures* 11.1–11.5 *and correspond to $\delta = 0$, $\gamma \geq 2$, $1 < \gamma < 2$, $0 < \gamma < 1$ and $\gamma < 0$, respectively.*

Theorem 2. *Any quadratic system of finite multiplicity $m_f = 3$ and*

an $M_{1,2}^i$ type of infinite critical point can be transformed by a linear transformation into system (9):

$$\dot{x} = \lambda x + \mu y + \gamma xy + \delta(x + y^2),$$
$$\dot{y} = x + y^2,$$

with $\lambda \in \{0,1\}$ and $\gamma \notin \{0,1\}$.

There are 119 topologically different phase portraits; they are given in Figures 10 and 11, together with the corresponding bifurcation diagrams.

System (9) has at most one limit cycle and, if it exists, it is hyperbolic.

APPENDIX

In this appendix the conditions on the coefficients in the general quadratic system (1) are derived, such that the system belongs to the classes studied in this paper.

It may be seen that $P_2(x,y) \equiv a_{20}x^2 + a_{11}xy + a_{02}y^2$ and $Q_2(x,y) \equiv b_{20}x^2 + b_{11}xy + b_{02}y^2$ have a common linear factor if and only if $A \equiv c_{46}^2 - c_{45}c_{56} = 0$, $c_{45}^2 + c_{46}^2 + c_{56}^2 \neq 0$, where $c_{45} \equiv a_{20}b_{11} - a_{11}b_{20}$, $c_{46} \equiv a_{20}b_{02} - a_{02}b_{20}$, $c_{56} \equiv a_{11}b_{02} - a_{02}b_{11}$, so that $c_{45} \neq 0$ and/or $c_{56} \neq 0$. It may be further deduced that for $c_{45} \neq 0$ this common linear factor is $c_{45}x + c_{46}y$, and for $c_{56} \neq 0$ it is equal to $c_{46}x + c_{56}y$.

If $c_{45} \neq 0$, apply to (1) the transformation

$$x = -c_{46}\bar{x} - c_{45}\bar{y},$$
$$y = c_{45}\bar{x} - c_{46}\bar{y},$$

to obtain, with $D = c_{45}^2 + c_{46}^2 \neq 0$,

(A1)
$$\begin{aligned}
D\dot{\bar{x}} &= \bar{x}' = \bar{a}_{00} + \bar{a}_{10}\bar{x} + \bar{a}_{01}\bar{y} + \bar{a}_{20}\bar{x}^2 + \bar{a}_{11}\bar{x}\bar{y} + \bar{a}_{02}\bar{y}^2 \\
&\equiv \bar{P}(\bar{x},\bar{y}), \\
D\dot{\bar{y}} &= \bar{y}' = \bar{b}_{00} + \bar{b}_{10}\bar{x} + \bar{b}_{01}\bar{y} + \bar{b}_{20}\bar{x}^2 + \bar{b}_{11}\bar{x}\bar{y} + \bar{b}_{02}\bar{y}^2 \\
&\equiv \bar{Q}(\bar{x},\bar{y}),
\end{aligned}$$

where

$$\bar{a}_{00} = -c_{46}a_{00} + c_{45}b_{00},$$

$$\bar{a}_{10} = c_{46}^2 a_{10} - c_{45}c_{46}a_{01} - c_{45}c_{46}b_{10} + c_{45}^2 b_{01},$$

$$\bar{a}_{01} = -c_{45}c_{46}a_{10} - c_{46}^2 a_{01} + c_{45}^2 b_{01} + c_{45}c_{46}b_{01},$$

$$\bar{a}_{20} = -c_{46}^3 a_{20} + c_{45}c_{46}^2 a_{11} - c_{45}^2 c_{46}a_{02} + c_{45}c_{46}^2 b_{20}$$
$$\qquad - c_{45}^2 c_{46}b_{11} + c_{45}^3 b_{02},$$

$$\bar{a}_{11} = 2c_{45}c_{46}^2 a_{20} - (c_{45}^2 - c_{46}^2)c_{46}a_{11} - 2c_{45}c_{46}^2 a_{02}$$
$$\qquad - 2c_{45}^2 c_{46}b_{20} + (c_{45}^2 - c_{46}^2)c_{45}b_{11} + 2c_{45}^2 c_{46}b_{02},$$

$$\bar{a}_{02} = -c_{45}^2 c_{46}a_{20} - c_{45}c_{46}^2 a_{11} - c_{46}^3 a_{02} + c_{45}^3 b_{20}$$
$$\qquad + c_{45}^2 c_{46}b_{11} + c_{45}c_{46}^2 b_{02},$$

$$\bar{b}_{00} = c_{45}a_{00} + c_{46}b_{00},$$

$$\bar{b}_{10} = -c_{45}c_{46}a_{10} + c_{45}^2 a_{01} - c_{46}^2 b_{10} + c_{45}c_{46}b_{01}$$

$$\bar{b}_{01} = c_{45}^2 a_{10} + c_{45}c_{46}a_{01} + c_{45}c_{46}b_{01} + c_{46}^2 b_{01},$$

$$\bar{b}_{20} = -c_{45}c_{46}^2 a_{20} + c_{45}^2 c_{46}a_{11} - c_{45}^3 a_{02} - c_{46}^3 b_{20}$$
$$\qquad + c_{45}c_{46}^2 b_{11} - c_{45}^2 c_{46}b_{02},$$

$$\bar{b}_{11} = -2c_{45}^2 c_{46}a_{20} + (c_{45}^2 - c_{46}^2)c_{45}a_{11} + 2c_{45}^2 c_{46}a_{02}$$
$$\qquad - 2c_{45}c_{46}^2 b_{20} + (c_{45}^2 - c_{46}^2)c_{46}b_{11} + 2c_{45}c_{46}^2 b_{02},$$

$$\bar{b}_{02} = c_{45}^3 a_{20} + c_{45}^2 c_{46}a_{11} + c_{45}c_{46}^2 a_{02} + c_{45}^2 c_{46}b_{20}$$
$$\qquad + c_{45}c_{46}^2 b_{11} + c_{46}^3 b_{02}.$$

If $c_{56} \neq 0$, by a similar transformation, (A1) may again be obtained, where now

$$\bar{a}_{00} = c_{56}a_{00} - c_{46}b_{00},$$

$$\bar{a}_{10} = c_{56}^2 a_{10} - c_{46}c_{56}a_{01} - c_{46}c_{56}b_{10} + c_{46}^2 b_{01},$$

$$\bar{a}_{01} = c_{46}c_{56}a_{10} + c_{56}^2 a_{01} - c_{46}^2 b_{01} - c_{46}c_{56}b_{01},$$

$$\bar{a}_{20} = c_{56}^3 a_{20} - c_{46}c_{56}^2 a_{11} + c_{46}^2 c_{56}a_{02} - c_{46}c_{56}^2 b_{20}$$
$$\qquad + c_{46}^2 c_{56}b_{11} - c_{46}^3 b_{02},$$

$$\bar{a}_{11} = 2c_{46}c_{56}^2 a_{20} + (c_{56}^2 - c_{46}^2)c_{56}a_{11} - 2c_{46}c_{56}^2 a_{02}$$
$$\qquad - 2c_{46}^2 c_{56}b_{20} - (c_{56}^2 - c_{46}^2)c_{46}b_{11} + 2c_{46}^2 c_{56}b_{02},$$

$$\bar{a}_{02} = c_{46}^2 c_{56}a_{20} + c_{46}c_{56}^2 a_{11} + c_{56}^3 a_{02} - c_{46}^3 b_{20}$$
$$\qquad - c_{46}^2 c_{56}b_{11} - c_{46}c_{56}^2 b_{02},$$

$$\bar{b}_{00} = c_{46}a_{00} + c_{56}b_{00},$$

$$\bar{b}_{10} = c_{46}c_{56}a_{10} - c_{46}^2 a_{01} + c_{56}^2 b_{10} - c_{46}c_{56}b_{01},$$
$$\bar{b}_{01} = c_{46}^2 a_{10} + c_{46}c_{56}a_{01} + c_{46}c_{56}b_{10} + c_{56}^2 b_{01},$$
$$\bar{b}_{20} = c_{46}c_{56}^2 a_{20} - c_{46}^2 c_{56}a_{11} + c_{46}^3 a_{02} + c_{56}^3 b_{20}$$
$$\qquad - c_{46}c_{56}^2 b_{11} + c_{46}^2 c_{56}b_{02},$$
$$\bar{b}_{11} = 2c_{46}^2 c_{56}a_{20} + (c_{56}^2 - c_{46}^2)c_{46}a_{11} - 2c_{46}^2 c_{56}a_{02}$$
$$\qquad + 2c_{46}c_{56}^2 b_{20} + (c_{56}^2 - c_{46}^2)c_{56}b_{11} - 2c_{46}c_{56}^2 b_{02},$$
$$\bar{b}_{02} = c_{46}^3 a_{20} + c_{46}^2 c_{56}a_{11} + c_{46}c_{56}^2 a_{02} + c_{46}^2 c_{56}b_{20}$$
$$\qquad + c_{46}c_{56}^2 b_{11} + c_{56}^3 b_{02}.$$

It may be seen that the common factor of $\bar{P}_2(\bar{x}, \bar{y}) \equiv \bar{a}_{20}\bar{x}^2 + \bar{a}_{11}\bar{x}\bar{y} + \bar{a}_{02}\bar{y}^2$ and $\bar{Q}_2(\bar{x}, \bar{y}) \equiv \bar{b}_{20}\bar{x}^2 + \bar{b}_{11}\bar{x}\bar{y} + \bar{b}_{02}\bar{y}^2$ is $\bar{y}$.

In fact, if $c_{45} \neq 0$, we may write

$$\bar{a}_{20} = -c_{46}(c_{46}^2 a_{20} - c_{45}c_{46}a_{11} + c_{45}^2 a_{02})$$
$$\qquad + c_{45}(c_{46}^2 b_{20} - c_{45}c_{46}b_{11} + c_{45}^2 b_{02}) = 0,$$
$$\bar{b}_{20} = -c_{45}(c_{46}^2 a_{20} - c_{45}c_{46}a_{11} + c_{45}^2 a_{02})$$
$$\qquad - c_{46}(c_{46}^2 b_{20} - c_{45}c_{46}b_{11} + c_{45}^2 b_{02}) = 0,$$

since $c_{45}x + c_{46}y$ is a factor of $P_2(x, y)$ and $Q_2(x, y)$, and the same follows if $c_{56} \neq 0$.

The critical points at infinity of (A1) are in the directions $\bar{y} = \bar{u}\bar{x}$, where $\bar{u}$ satisfies

$$f(\bar{u}) \equiv \bar{a}_{02}\bar{u}^3 + (\bar{a}_{11} - \bar{b}_{02})\bar{u}^2 + (\bar{a}_{20} - \bar{b}_{11})\bar{u} - \bar{b}_{20} = 0.$$

The transversally nonhyperbolic point at $\bar{u} = 0$ is third order in the direction of the Poincaré circle if $\bar{b}_{11} = 0$, $\bar{a}_{11} = \bar{b}_{02} \neq 0$, $\bar{a}_{02} \neq 0$. In order that (A1) is of class $m_f = 3$, there should be $\bar{b}_{10} \neq 0$ since $\bar{b}_{10} = 0$ yields $m_f \leq 2$. Elimination of $\bar{x}$ between $\bar{P}(\bar{x}, \bar{y}) = 0$ and $\bar{Q}(\bar{x}, \bar{y}) = 0$ yields an equation for the coordinate $\bar{y}$ of a finite critical point of third degree if $\bar{b}_{10} \neq 0$, thus this condition is also sufficient.

In summary, a quadratic system is of the class $m_f = 3$ with an infinite critical point of type $M_{1,3}^i$, if the following conditions are satisfied:

$$A \equiv c_{46}^2 - c_{45}c_{56} = 0, \qquad c_{45}^2 + c_{46}^2 + c_{56}^2 \neq 0,$$
$$\bar{b}_{11} = 0, \qquad \bar{a}_{11} = \bar{b}_{02} \ (\neq 0), \qquad \bar{b}_{10} \neq 0, \qquad \bar{a}_{02} \neq 0.$$

Similarly, it can be derived that if a quadratic system is of the class $m_f = 3$ with an infinite critical point of type $M_{1,2}^i$ that the following conditions should be satisfied: $A \equiv c_{46}^2 - c_{45}c_{56} = 0$, $c_{45}^2 + c_{46}^2 + c_{56}^2 \neq 0$, $\bar{b}_{11} = 0$, $\bar{a}_{11} \neq \bar{b}_{02}(\bar{a}_{11}\bar{b}_{02} \neq 0)$, $\bar{b}_{10} \neq 0$.

REFERENCES

1. A.A. Andronov, E.A. Leontovich, J.J. Gordon and A.G. Maier, *Qualitative theory of second-order dynamic systems*, Israel Program for Scientific Translations, Jerusalem, Wiley, New York, 1973.

2. ———, *Theory of bifurcations of dynamic systems on a plane*, Israel Program for Scientific Translations, Jerusalem, Wiley, New York, 1973.

3. R.I. Bogdanov, *Versal deformation of a singularity of a vector field on the plane in the case of zero eigenvalues*, Select Math. Sov. **1** (1981), 389–421.

4. D. Bularas, N.I. Vulpe and K.S. Sibirskii, *The problem of a center 'in the large' for a general quadratic system*, Dokl. Akad. Nauk SSSR **311** (1990), 4, Soviet Math. Dokl. **41** (1990), 287–290.

5. Li Chengzhi, J. Llibre and Zhang Zhifen, *Weak focus, limit cycles and bifurcations for bounded quadratic systems*, J. Differential Equations **115** (1995), 193–223.

6. B. Coll, A. Gasull and J. Llibre, *Some theorems on the existence, uniqueness and non-existence of limit cycles for quadratic systems*, J. Differential Equations **67** (1987), 372–399.

7. W.A. Coppel, *A new class of quadratic systems*, J. Differential Equations **92** (1991), 360–372.

8. ———, *Some quadratic systems with at most one limit cycle*, Dynam. Report. Ser. Dynam. Syst. Appl. **2** (1989), 61–88.

9. R.J. Dickson and L.M. Perko, *Bounded quadratic systems in the plane*, J. Differential Equations **7** (1970), 251–273.

10. G.F.P. Duff, *Limit cycles and rotated vector fields*, Ann. Math. **57** (1953), 15–31.

11. X. Huang and J.W. Reyn, *On the distribution of limit cycles in quadratic systems with finite multiplicity three*, Reports of the Faculty of Mathematics and Informatics, 94-109, Delft University of Technology (1994), 43 pp.

12. J. Hulshof, *Similarity solutions of the porous medium equation with sign changes*, Appl. Math. Lett. **2** (1989), 229–232.

13. D.S. Malkus, J.A. Nohel and B.J. Plohr, *Analysis of new phenomena in shear flow of non-Newtonian fluids*, SIAM J. Appl. Math. **51** (1991), 899–929.

14. L.M. Perko, *Rotated vector fields*, J. Differential Equations **103** (1993), 127–145.

15. J.W. Reyn, *A bibliography of the qualitative theory of quadratic systems of differential equations in the plane*, Reports of the Faculty of Mathematics and Informatics, 94-02, Delft University of Technology, 3rd edition (1994).

16. ———, *On defining classes of quadratic systems in the plane*, Reports of the Faculty of Mathematics and Informatics, 91-32, Delft University of Technology (1991), 35 pp.

17. J.W. Reyn, *Classes of quadratic systems of differential equations in the plane*, Nakai Ser. Pure Appl. Math. Theor. Physics **4**, Dynamical Systems (1993), 146–180.

18. ———, *Phase portraits of quadratic systems without finite critical points*, Nonlinear Anal. Theory Methods Appl. **27** (1996), 207–222.

19. ———, *Phase portraits of non degenerate quadratic systems with finite multiplicity one*, Nonlinear Anal. Theory Methods Appl. **28** (1997), 755–778.

20. D. Schlomiuk, *Algebraic particular integrals, integrability and the problem of the center*, Trans. Amer. Math. Soc. **338** (1993), 799–841.

21. Ye Yanqian, et al., *Theory of limit cycles*, Trans. Math. Mon. **66** (1986), 415.

DELFT UNIVERSITY OF TECHNOLOGY, FACULTY OF TECHNICAL MATHEMATICS AND INFORMATICS, MEKELWEG 4, 2628 CD DELFT, THE NETHERLANDS